

CHEMISTRY

A European Journal

A Journal of



Accepted Article

Title: Perfluoroalkyltricyanoborate and Perfluoroalkylcyanofluoroborate Anions: Building Blocks for Low-viscosity Ionic Liquids

Authors: Johannes Landmann, Jan A. P. Sprenger, Philipp T. Hennig, Rüdiger Bertermann, Matthias Grüne, Frank Würthner, Nikolai V. Ignat'ev, and Maik Finze

This manuscript has been accepted after peer review and appears as an Accepted Article online prior to editing, proofing, and formal publication of the final Version of Record (VoR). This work is currently citable by using the Digital Object Identifier (DOI) given below. The VoR will be published online in Early View as soon as possible and may be different to this Accepted Article as a result of editing. Readers should obtain the VoR from the journal website shown below when it is published to ensure accuracy of information. The authors are responsible for the content of this Accepted Article.

To be cited as: *Chem. Eur. J.* 10.1002/chem.201703685

Link to VoR: <http://dx.doi.org/10.1002/chem.201703685>

Supported by
ACES

WILEY-VCH

Perfluoroalkyltricyanoborate and Perfluoroalkylcyanofluoroborate Anions: Building Blocks for Low-viscosity Ionic Liquids

Johannes Landmann,^[a] Jan A. P. Sprenger,^[a] Philipp T. Hennig,^[a] Rüdiger Bertermann,^[a] Matthias Grüne,^[b] Frank Würthner,^[b] Nikolai V. Ignat'ev,^[a,c] and Maik Finze^{*,[a]}

Abstract: Potassium perfluoroalkyltricyanoborates $K[C_nF_{2n+1}B(CN)_3]$ ($n = 1$ (**1d**), 2 (**2d**)) and potassium mono(perfluoroalkyl)cyanofluoroborates $K[C_nF_{2n+1}BF(CN)_2]$ ($n = 1$ (**1c**), 2 (**2c**)) and $[C_nF_{2n+1}BF_2(CN)]^-$ ($n = 1$ (**1b**), 2 (**2b**), 3 (**3b**), 4 (**4b**)) are accessible with perfect selectivities on multi-gram scales starting from $K[C_nF_{2n+1}BF_3]$ and Me_3SiCN . The K^+ salts are starting materials for the preparation of salts with organic cations, e.g. $[EMIm]^+$ (EMIm = 1-ethyl-3-methylimidazolium). These $[EMIm]^+$ salts are hydrophobic room temperature ionic liquids (RTILs) that are thermally, chemically, and electrochemically very robust, offering electrochemical windows of up to 5.8 V. The RTILs described exhibit very low viscosities with a minimum of 14.0 mPa·s at 20 °C for $[EMIm]^+1c$, low melting points of

down to -57 °C for $[EMIm]^+2b$, and extraordinary high conductivities of up to 17.6 mS·cm⁻¹ at 20 °C for $[EMIm]^+1c$. The combination of properties makes these ILs promising materials for electrochemical devices as exemplified by the application of selected RTILs as component of electrolytes in dye-sensitized solar cells (DSSCs, Grätzel cells). The efficiency of the DSSCs was found to increase with decreasing viscosity of the neat ionic liquid. In addition to the spectroscopic characterization, single crystals of the potassium salts of **1b–d**, **2d**, **3b** and **4c** as well as of $[nBu_4N]^+2c$ have been studied by X-ray diffraction.

Introduction

Cyanoborate anions are an emerging class of building blocks especially for room temperature ionic liquids (RTILs).^[1] RTILs are of growing importance for fundamental and applied science ranging from pharmaceuticals, biochemistry, chemistry to physics, and engineering.^[2] The archetype cyanoborate anion is the tetracyanoborate anion $[B(CN)_4]^-$ (**TCB**, Figure 1),^[3–5] which gives low-melting and low-viscosity ionic liquids that are chemically and electrochemically very stable and thermally robust.^[1,5,6] Many physicochemical properties of **TCB**-ILs were studied experimentally and by theoretical methods.^[1,7] For example, the RTILs $[EMIm]^+TCB$ (EMIm = 1-ethyl-3-methylimidazolium) and $[BMPL]^+TCB$ (BMPL = 1-butyl-1-methylpyrrolidinium) have been used in electrolyte compositions for electrochemical devices such as dye-sensitized solar cells (DSSCs, Grätzel cells).^[8,9] Similarly, mixed cyanofluoro- $[BF_{4-x}(CN)_x]^-$ and cyanohydridoborate anions $[BH_{4-x}(CN)_x]^-$ ($x = 1–3$) have been successfully applied in RTILs that have even lower melting points and lower viscosities than the corresponding **TCB**-IL, which is mostly due to the lower symmetry and the reduced molecular weight of the heteroleptic borate anions.^[1] In the series $[EMIm]^+[BF_{4-x}(CN)_x]^-$ and $[EMIm]^+[BH_{4-x}(CN)_x]^-$ ($x = 0–4$) the tricyanoborate-ILs $[EMIm]^+[BF(CN)_3]^-$ ($[EMIm]^+MFB$, Figure 1) and

$[EMIm]^+[BH(CN)_3]^-$ provide the best compromise in hydrophobicity low melting point, low viscosity, and chemical, thermal as well as electrochemical stability.^[1] These properties are requirements for ILs used in electrochemical devices. The $[EMIm]^+$ salts of $[BF_2(CN)_2]^-$ and $[BH_2(CN)_2]^-$ have lower melting points and viscosities than $[EMIm]^+[BX(CN)_3]^-$ ($X = F, H$) but they are more reactive and less stable and their hydrophobic nature is less distinct.^[1,10] In addition to applications in ILs, cyanoborate anions are used as counteranions for metal and main group element cations. E.g. redox couples^[11] and luminescent materials^[12] based on the **TCB** anion have been developed, Ph_3CTCB was used in zirconium chemistry^[13] and $HTCB$ ^[14] is a superacid.^[15] Cyanoborates are starting materials for further borates, for example salts of $[(CF_3)_3B(CN)]^-$ (**I**, Figure 1),^[16] $[B(CF_3)_4]^-$ (**II**, Figure 1)^[16,17] and $[B(CO_2H)_4]^-$ ^[18] were prepared from tetracyanoborates. $B(CN)_3^{2-}$ has become accessible from salts of $[BX(CN)_3]^-$ ($X = CN$ (**TCB**),^[19] F (**MFB**),^[20] H ^[21]) and $[B_2(CN)_6]^{2-}$ from **MFB**-salts.^[22]

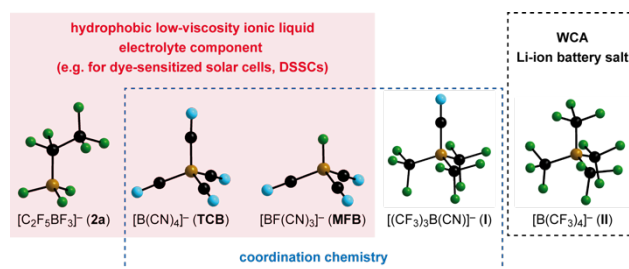


Figure 1. Selected cyano- and perfluoroalkylborate anions and most relevant fields of applications.

Perfluoroalkylborate anions^[23–25] are another important class of anions that are of interest for catalysis, materials science and organic synthesis. The tetrakis(trifluoromethyl)borate anion $[B(CF_3)_4]^-$ (**II**, Figure 1)^[16,17,26] is a very weakly coordinating anion^[24,27] that was used for the stabilization of reactive cations such as $[Ag(CO)_4]^+$,^[17] $[Au(NCMe)_2]^+$,^[28] $[Co(CO)_5]^+$,^[29] N_5^+ ,^[30] NO^+ ,^[31] and $[H(OEt_2)_2]^+$.^[13] Furthermore, the $[B(CF_3)_4]^-$ anion is electrochemically very stable and solutions of its Li^+ salt reveal

[a] J. Landmann, Dr. J. A. P. Sprenger, P. T. Hennig, Dr. R. Bertermann, Dr. Nikolai V. Ignat'ev, Prof. Dr. M. Finze Julius-Maximilians-Universität Würzburg, Institut für Anorganische Chemie, Institut für nachhaltige Chemie & Katalyse mit Bor (ICB) Am Hubland, 97074 Würzburg, Germany E-mail: maik.finze@uni-wuerzburg.de <https://go.uni.wue.de/finze-group>

[b] Dr. M. Grüne, Prof. Dr. F. Würthner Julius-Maximilians-Universität Würzburg, Institut für Organische Chemie & Center for Nanosystems Chemistry, Am Hubland, 97074 Würzburg, Germany

[c] Dr. Nikolai V. Ignat'ev Consultant, Merck KGaA, Frankfurter Straße 250, 64293 Darmstadt, Germany

Supporting information for this article is given via a link at the end of the document.

high Li-ion conductivity.^[32] Anion **II** is the only tetrakis(perfluoroalkyl)borate anion known, to date.^[23–25] In contrast, a substantial number of borate anions with one, two and three perfluoroalkyl groups have been described.^[23–25] Especially, mono(perfluoroalkyl)borate anions with three fluoro or alkoxy groups have been studied.^[23,33,34] The physicochemical properties of RTILs with perfluoroalkyltrifluoroborate anions like $[\text{C}_2\text{F}_5\text{BF}_3]^-$ (**2a**, Figure 1) have been reported,^[35,36,37] and some anions have been studied as component in Li-ion electrolytes.^[38,39] Perfluoroalkyltrialkoxoborates are valuable starting materials for perfluoroalkyl transfer reactions in organic synthesis^[40] and for the preparation of the corresponding perfluoroalkyltrifluoroborates.^[23,37,39,41–43]

Little is known on borate anions containing both, cyano and perfluoroalkyl groups, in general. The tris(trifluoromethyl)cyanoborate anion $[(\text{CF}_3)_3\text{B}(\text{CN})]^-$ (**1**, Figure 1)^[16,44,45] was used in coordination^[28,46,47] and main group element chemistry.^[13,15,47] The high thermal and chemical stability of **1** points towards potential applications of mixed perfluoroalkylcyanoborates. Lanthanide frameworks with the pentafluoroethyltricyanoborate anion $[\text{C}_2\text{F}_5\text{B}(\text{CN})_3]^-$ (**2d**) are the only further examples for compounds containing mixed perfluoroalkylcyanoborate anions. However, no details on the synthesis of anion **2d** were given.^[48] Here, we report on the synthesis and spectroscopic as well as structural properties of potassium perfluoroalkyltricyanoborates and potassium mono(perfluoroalkyl)cyanofluoroborates that in part have been described in two patent applications, earlier.^[49,50] The potassium salts were used as starting materials for the preparation of salts with organic cations. The $[\text{EMIm}]^+$ salts are RTILs with promising properties that were characterized by spectroscopic, thermal and electrochemical methods, in detail.

Results and Discussion

Synthetic Aspects

Anion synthesis. Potassium perfluoroalkyltricyanoborates and potassium mono(perfluoroalkyl)cyanofluoroborates were obtained in excellent yield, with perfect selectivity, in high purity and on a large scale (up to 0.15 mol) starting from the respective perfluoroalkyltrifluoroborate and Me_3SiCN . The trimethylsilylcyanide can conveniently be synthesized *in situ* and used without purification for the preparation of the cyanoborates. The trimethylsilylcyanide served as reagent and solvent and the unreacted material was recovered and reused in subsequent syntheses. In Figure 2 the most important synthetic strategies are exemplified for the preparation of $\text{K}[\text{C}_2\text{F}_5\text{BF}_2(\text{CN})]$ (**K2b**), $\text{K}[\text{C}_2\text{F}_5\text{BF}(\text{CN})_2]$ (**K2c**) and $\text{K}[\text{C}_2\text{F}_5\text{B}(\text{CN})_3]$ (**K2d**) (Figure 2). The unprecedentedly high selectivity of the successive exchange of fluorine against cyano substituents is demonstrated by the ^{11}B , ^{19}F , and ^{13}C NMR spectra of the four salts in Figure 3 and it is important to note that the ^{11}B and ^{19}F NMR spectra have been recorded on samples of the reaction mixtures.

The perfluoroalkylcyanodifluoroborates $\text{K}[\text{R}^{\text{F}}\text{BF}_2(\text{CN})]$ were obtained either in neat Me_3SiCN by heating or microwave irradiation (entries **A** and **C**) or in a mixture of Me_3SiCN and Me_3SiCl (entry **B**). The trimethylsilylchloride acts as Lewis acid catalyst and enables lower reaction temperatures. E.g. the addition of ca. 7 vol-% of Me_3SiCl resulted in full conversion of **2a** into **2b** within minutes at room temperature, whereas more than 50 °C were necessary for reactions without Me_3SiCl . A related Me_3SiCl -catalysed cyanation was established for the synthesis of

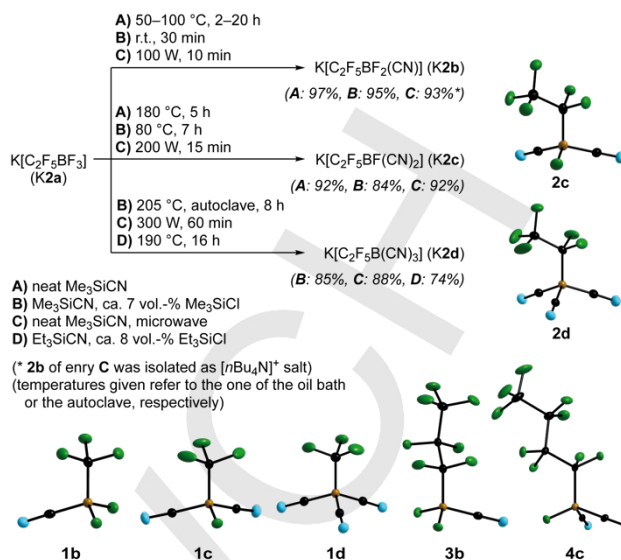


Figure 2. Selected optimized syntheses of $\text{K}[\text{C}_2\text{F}_5\text{BF}_{3-x}(\text{CN})_x]$ ($x = 1$: **K2b**; $x = 2$: **K2c**; $x = 3$: **K2d**) and molecular structures of selected cyanoborate anions (displacement ellipsoids at the 50% probability level for **K1b**, **K1d**, **K3b**-0.33 Me_2CO or at the 25% probability level for **K1c**, **K2d**, $[\text{nBu}_4\text{N}]\text{2c}$ and **K4c**- Me_2CO).

salts of the $[\text{BF}(\text{CN})_3]^-$ anion starting from alkali metal tetrafluoroborates.^[51] Another synthesis towards **K2b** started from **K2a**, LiCl , and KCN . The solids were pestled and heated to 180 °C for 20 hrs resulting in a mixture of 82% of **2b** and 18% of further borate anions (see Supporting Information). This method is similar to the synthesis of **KTcB** using $\text{K}[\text{BF}_4]$, KCN and LiCl .^[5]

In case of potassium mono(perfluoroalkyl)dicyanofluoroborates $\text{K}[\text{R}^{\text{F}}\text{BF}(\text{CN})_2]$ harsher conditions had to be applied to achieve the exchange of a second fluorine substituent against a cyano group. **K2c** was obtained in neat Me_3SiCN at 180 °C in a closed reaction vessel after 5 hrs (entry **A**). The conversion of **2a** into **2c** was achieved at 150 °C, as well, but with a reaction time of 42 h. Attempted synthesis of **K2c** in an open vessel under reflux remained unsuccessful, which is rationalized by (i) the lower reaction temperature ($T_{\text{bp}}(\text{Me}_3\text{SiCN}) = 117.2\text{ °C}^{[52]}$) and (ii) by loss of the volatile by-product Me_3SiF ($T_{\text{bp}}(\text{Me}_3\text{SiF}) = 16\text{ °C}^{[52]}$). Me_3SiF promotes the transformation as a weak Lewis acid as demonstrated by reactions of $\text{K}[\text{C}_6\text{F}_5\text{BF}_3]$ with and without trimethylsilyl fluoride (Figure S1 in the Supporting Information). The addition of Me_3SiCl resulted in a significant reduction of the temperature, for example **K2a** was transformed into **K2c** already at 80 °C (entry **B**). During the synthesis of salts of perfluoroalkylidicyanofluoroborate anions, the corresponding perfluoroalkylcyanofluoroisocyanoborate anions were identified as intermediates, which is a result of the relatively low reaction temperature that is not sufficient for the isomerization of the isocyno- to the cyanoborate. Figure S7 in the Supporting Information shows representative ^{11}B , ^{13}C , and ^{19}F NMR spectra of a reaction mixture that contained minor amounts of the anions $[\text{C}_2\text{F}_5\text{BF}_2(\text{CN})]^-$ (**2b**) and $[\text{C}_2\text{F}_5\text{BF}(\text{CN})_2]^-$ (**2c**) along with the major component $[\text{C}_2\text{F}_5\text{BF}(\text{NC})(\text{CN})]^-$, which at higher temperatures isomerizes to the dicyanoborate anion **2c**. Earlier, the formation of isocyanoborate intermediates was described for the synthesis of $[\text{BF}(\text{CN})_3]^-$, earlier.^[51] The potassium salt of anion **2c** was prepared via a microwave assisted reaction in neat Me_3SiCN , as well (entry **C**). Although the microwave-assisted synthesis

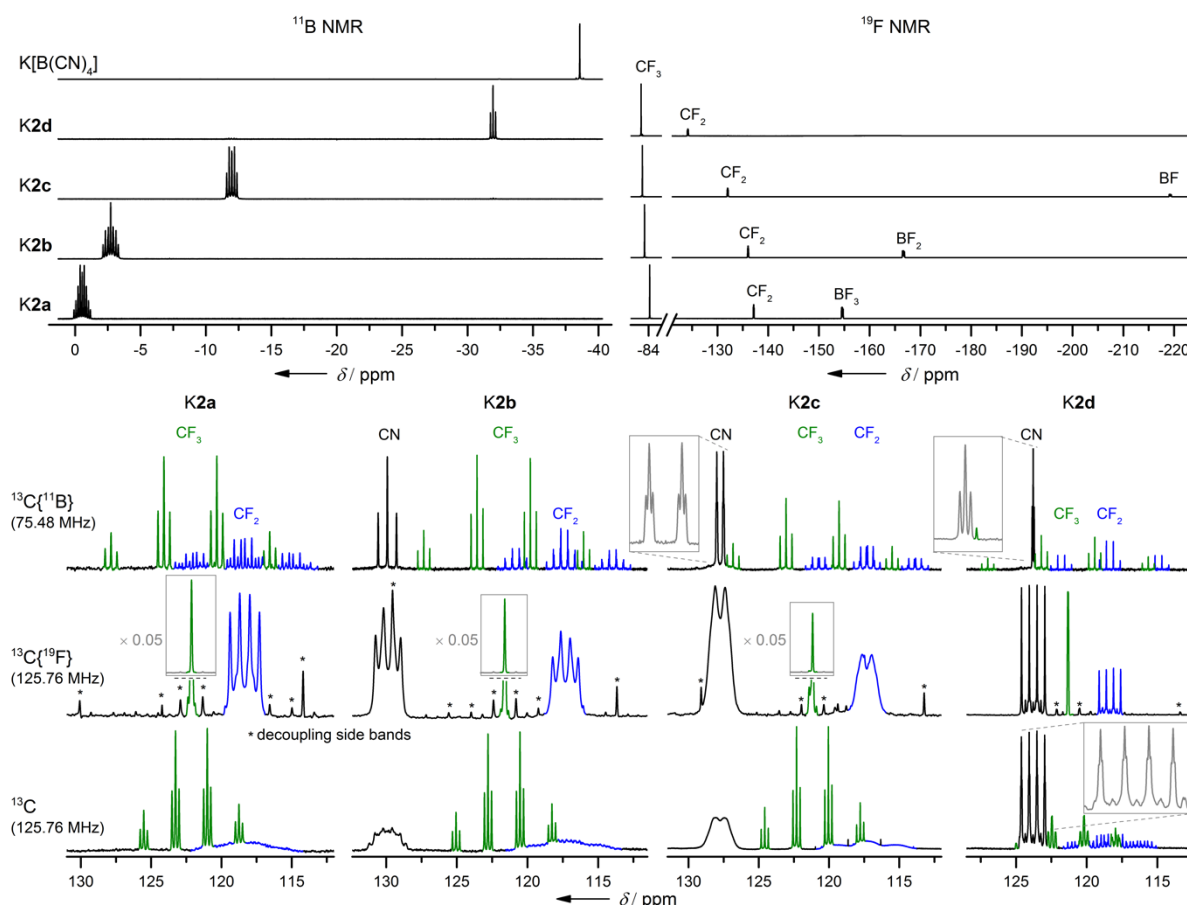


Figure 3. ^{11}B , ^{19}F and ^{13}C NMR spectra of the anions $[\text{C}_2\text{F}_5\text{B}(\text{CN})_3]^-$ (**2d**), $[\text{C}_2\text{F}_5\text{BF}(\text{CN})_2]^-$ (**2c**), $[\text{C}_2\text{F}_5\text{BF}_2(\text{CN})]^-$ (**2b**), $[\text{C}_2\text{F}_5\text{BF}_3]^-$ (**2a**), as well as the ^{11}B NMR spectrum of the anion $[\text{B}(\text{CN})_4]^-$ (**TCB**).

is by far the fastest reaction, the Me_3SiCl -catalysed process is the method of choice as it easily enables reactions on larger scales.

The exchange of the last fluorine substituent at boron to yield the respective perfluoroalkyltricyanoborates $\text{K}[\text{R}^{\text{F}}\text{B}(\text{CN})_3]$ required even harsher conditions (Figure 2). The most convenient entry towards $\text{K}[\text{R}^{\text{F}}\text{B}(\text{CN})_3]$ is again the Me_3SiCl -catalyzed reaction that was performed at 205 °C in an autoclave as exemplified for **K2d** (entry **B**). The related synthesis without Me_3SiCl started at temperatures higher than 250 °C but the mixture contained a number of unidentified side- and decomposition products. Thus, the procedure was not optimized and is not included in Figure 2. A technical disadvantage is the high pressure of the synthesis in Me_3SiCN with Me_3SiCl . This disadvantage was circumvented by the use of high-boiling Et_3SiCN and Et_3SiCl (entry **D**; $T_{\text{bp}}(\text{Et}_3\text{SiCN}) = 180\text{--}182\text{ °C}$,^[53] $T_{\text{bp}}(\text{Et}_3\text{SiCl}) = 144\text{--}146\text{ °C}$,^[54] $T_{\text{bp}}(\text{Et}_3\text{SiF}) = 109\text{ °C}$ ^[55]). However, Et_3SiCN is commercially not available and Et_3SiCl is more expensive than Me_3SiCl . An alternative approach is again a microwave assisted synthesis in neat Me_3SiCN that gave pure $\text{K}[\text{C}_2\text{F}_5\text{B}(\text{CN})_3]$ (**K2d**) but high pressure has to be considered for this transformation (entry **C**).

The crude potassium salts that have been obtained after removal of all volatiles, contain small amounts of polymeric organic impurities. Especially, tricyanoborates are brownish to black, which is due to the harsh reaction conditions required. However, these impurities are easily removed by treatment with hydrogen peroxide (up to 30% v/v) and K_2CO_3 to give the

potassium salts after precipitation from e.g. a solution in THF by the addition of dichloromethane. The resistance of the cyanoborates against peroxides exemplifies their chemical robustness. In addition, the salts $\text{K}[\text{R}^{\text{F}}\text{BF}_{3-x}(\text{CN})_x]$ ($x = 1\text{--}3$) are indefinitely stable at room temperature in air.

Ionic liquid (IL) synthesis. The potassium salts of the perfluoroalkyltricyanoborate and mixed mono(perfluoroalkyl)cyanoboroborate anions have been converted into salts with organic cations in moderate to excellent yields, mostly >80%. The metatheses were performed in aqueous solutions and the hydrophobic organic salts were isolated either by (i) phase separation, (ii) filtration, or (iii) extraction with dichloromethane. The $[\text{EMIm}]^+$ salts are RTILs that have been washed with deionized water in order to remove traces of halides. The ILs were dried in a vacuum overnight at slightly elevated temperatures to remove traces of water. The water content was below 50 ppm as assessed by Karl-Fischer titration.

Structural and spectroscopic characterization

X-ray diffraction. Colourless single crystals of **K1b**, **K1c**, **K1d**, **K2d**· Me_2CO , $[\text{nBu}_4\text{N}]\text{2c}$, **K3b**· $0.33\text{Me}_2\text{CO}$, and **K4c**· Me_2CO suitable for X-ray diffraction were obtained from acetone solutions by slow evaporation of the solvent (Figure 2, Table 1, Table S6 and S7 in the Supporting Information). The bond parameters of the new anions are similar to values reported for other perfluoroalkylborate and cyanoborate anions, e.g. $[\text{R}^{\text{F}}\text{BF}_3]^-$ ($\text{R}^{\text{F}} = \text{CF}_3$ (**1a**),^[56] C_2F_5 (**2a**)^[57]) $[(\text{CF})_3\text{B}(\text{CN})]^-$ (**I**),^[44] $[\text{B}(\text{CN})_4]^-$ (**TCB**)^[3] and $[\text{BF}(\text{CN})_3]^-$ (**MFB**).^[51]

Table 1. Selected experimental and calculated^[a] bond parameters and spectroscopic data of [CF₃BF_{3-x}(CN)_x]⁻ (**1a-d**).^[b]

		[CF ₃ BF ₃] ⁻ (1a)		[CF ₃ BF ₂ (CN)] ⁻ (1b)		[CF ₃ BF(CN) ₂] ⁻ (1c)		[CF ₃ B(CN) ₃] ⁻ (1d)	
		exptl	calcd	exptl	calcd	exptl	calcd	exptl	calcd
<i>d</i> (B–F)	[pm]	139.1(5)	141.2	139.7(2)	141.2	139.8(3)	142.0	–	–
<i>d</i> (B–CN)	[pm]	–	–	163.0(2)	162.4	161.0(3)	160.6	160.1(2)	159.1
<i>d</i> (B–CF ₃)	[pm]	162.5(6)	165.7	163.0(2)	165.2	162.3(4)	164.7	163.2(2)	164.5
<i>d</i> (C≡N)	[pm]	–	–	114.3(2)	115.7	114.2(3)	115.6	114.7(2)	115.6
<i>d</i> (C–F)	[pm]	134.3(8)	137.6	135.7(2)	137.1	133.3(3)	136.8	135.3(2)	136.5
$\tilde{\nu}$ (CN)	[cm ⁻¹]	–	–	2209	2301	2214	2306	2223	2314
δ (¹¹ B)	[ppm]	–1.3	–2.0	–3.8	–5.7	–12.8	–16.3	–32.0	–36.4
δ (¹⁹ F) BF	[ppm]	–156.6	–195.5	–169.2	–203.9	–219.9	–256.1	–	–
δ (¹⁹ F) CF ₃	[ppm]	–76.1	–98.4	–77.5	–100.0	–74.0	–95.9	–66.4	–87.3
δ (¹³ C) CN	[ppm]	–	–	129.8	134.6	127.8	132.9	123.6	129.0
δ (¹³ C) CF ₃	[ppm]	131.4	145.5	130.0	144.1	130.1	144.1	130.0	144.1
¹ <i>J</i> (¹⁹ F, ¹¹ B)	[Hz]	39.6	–101.5	48.8	–108.2	49.1	–105.6	–	–
¹ <i>J</i> (¹³ C, ¹¹ B) B–CN	[Hz]	–	–	75.3	82.9	71.3	77.0	69.4	72.8
¹ <i>J</i> (¹³ C, ¹¹ B) B–CF ₃	[Hz]	110.1	112.5	97.8	98.4	88.3	87.9	80.6	80.2
¹ <i>J</i> (¹⁹ F, ¹³ C)	[Hz]	310.8	–385.6	308.1	–382.1	305.4	–377.5	301.7	–373.0
² <i>J</i> (¹⁹ F, ¹³ C) F–B–CN	[Hz]	–	–	48.7	45.2	35.7	32.1	–	–
² <i>J</i> (¹⁹ F, ¹³ C) F–B–CF ₃	[Hz]	66.7	64.4	43.3	41.0	31.8	28.6	–	–

[a] B3LYP/6-311++G(d); NMR parameters: B3LYP/6-311++G(2d) using the geometries calcd at the B3LYP/6-311++G(d) level of theory. [b] NMR solvent: (CD₃)₂CO; IR data: neat [EMIm]⁺ salt; bond distances and NMR data: K⁺ salts.

According to the X-ray diffraction data, *d*(B–F) increases and *d*(B–CN) decreases with increasing content of cyano groups in the series of trifluoromethylborate anions [CF₃BF_{3-x}(CN)_x]⁻ (*x* = 0–3; **1a-d**; Table 1). Although the differences are small and not all are significant (<3σ) they are in excellent agreement to theoretical data. Both trends indicate stronger B–CN and weaker B–F bond(s) with increasing number of cyano groups. The experimentally determined distances *d*(B–CF₃), *d*(C–F), and *d*(C≡N) do not show any explicit trend but DFT calculations predict shorter bonds with increasing number of cyano groups.

The pentafluoroethylborate anions **2a-d** reveal an analogous behaviour for the bond lengths as the ones discussed for the trifluoromethylborate anions **1a-d** (Table S7 in the Supporting Information). Furthermore, an increasing length of the perfluoroalkyl chain does not significantly influence the B–CN and B–F bond distances. The B–CF_{2/3} distance is marginally elongated for anions with longer perfluoroalkyl chains (**1c**: 162.3(4), **2c**: 163.6(6), and **4c**: 165.4(4) pm).

Vibrational spectroscopy. The slightly shorter C≡N distance predicted by DFT calculations is an indication for a stronger C≡N bond that is supported by $\tilde{\nu}$ (CN) of the EMIm-ILs by increasing wavenumbers in the same order. The larger $\tilde{\nu}$ (CN) reflect the ascending Lewis acidity of the corresponding boranes CF₃BF_{2-x}(CN)_x (*x* = 0–2, *vide infra*). Thus, $\tilde{\nu}$ (CN) of [(CF₃)₃B(CN)]⁻ (**1d**) is the highest value with 2244 cm⁻¹ that has been reported for a cyanoborate anion, so far.^[44] Again, this high wavenumber correlates with *d*(B–CN) of [(CF₃)₃B(CN)]⁻ of 158.9(3) pm^[44] that is significantly shorter than the one of **1d** (160.1(2) pm). Both findings display the high Lewis acidity of (CF₃)₃B,^[24,58] which leads to a strengthening of the B–CN and C≡N bond, alike.

NMR spectroscopy. All new perfluoroalkylcyanoborate anions [R^FBF_{3-x}(CN)_x]⁻ (*x* = 1–3) and the corresponding trifluoroborate anions were characterized by multinuclear NMR spectroscopy (Table S4 in the Supporting Information). δ (¹¹B) decreases in the series **1a-d** (Table 1) and **2a-d** (Figure 3) with increasing number of cyano groups. δ (¹⁹F) of the BF moiety reveals an analogous trend whereas the ¹⁹F resonance frequen-

cy of the CF_{2/3} unit that is bonded to boron shows the reverse trend with [CF₃BF₃]⁻ (**1a**) being the only exception. The difference in δ (¹⁹F) for the fluorine atoms at the CF_{2/3} units that are not directly attached to boron is much less pronounced as evident from the signal of the CF₃ unit of the pentafluoroethyl groups of anions **2a-d** in Figure 3.

The assignment of the strongly coupled ¹³C NMR spectra is aided by ¹⁹F and ¹¹B decoupling experiments as exemplified by the spectra of the pentafluoroethyl derivatives **2a-d** depicted in Figure 3. δ (¹³C) of the cyano groups follows a definite trend to smaller resonance frequencies with increasing number of CN groups (Table 1 and Figure 3). In contrast, the ¹³C NMR signals of the perfluoroalkyl groups are close and no obvious tendency is observed. In the ¹¹B coupled spectra of the anions [C₂F₅BF₂(CN)]⁻ (**2b**) and [C₂F₅BF(CN)₂]⁻ (**2c**) the signals of the CN and CF₂ group(s) are much broader than the respective signals of the anion [C₂F₅B(CN)₃]⁻ (**2d**). Similarly, the signal of the CF₂ group of [C₂F₅BF₃]⁻ (**2a**) is less broadened. The larger line width is paralleled by a distortion of the quartet that is due to ¹*J*(¹³C, ¹¹B) coupling. Both effects, broad lines and distorted multiplet, are a result of the interaction with the quadrupolar nucleus ¹¹B, which increases with decreasing local symmetry at boron.^[44,59] The ¹⁹F NMR signals of the F atoms and CF_{2/3} unit bonded to boron are affected by quadrupolar coupling in a similar way as the ¹³C signals. The line width of the ¹¹B signals shows the same behaviour, as well, but without any distortion of the multiplets.^[44,59]

Most of the coupling constants reveal definite trends (Table 1). For example, ¹*J*(¹³C, ¹¹B) of the B–CN and B–CF₃ moieties in **1a-d** decreases with increasing number of cyano groups.

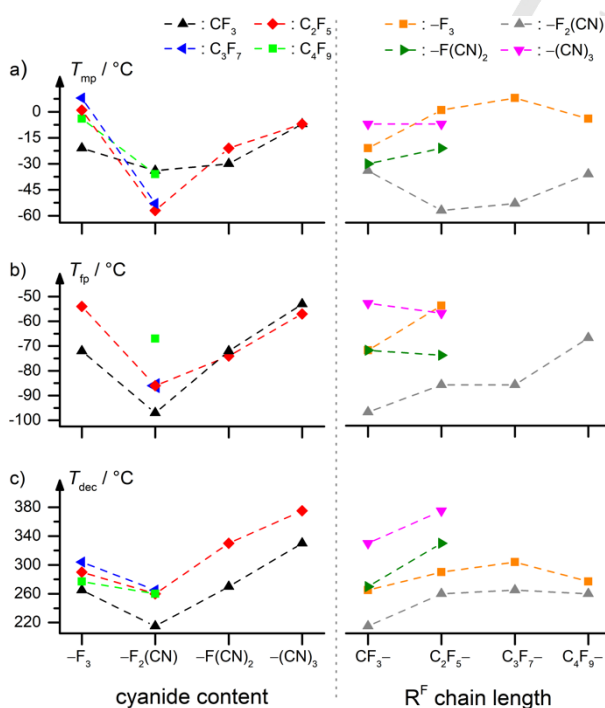
Thermal properties

EMIm-ILs. All salts [EMIm][R^FBF_{3-x}(CN)_x] (*x* = 1–3) are RTILs (Table 2). The melting points (*T*_{mp}) are mostly lower than the ones of [EMIm][R^FBF₃] and all are below those of [EMIm][BF₄] (15 °C)^[35] and [EMIm]TfCB (8 °C).^[1] [EMIm]II is a solid that melts at 125 °C. The lowest melting points for [EMIm][R^FBF_{3-x}(CN)_x] have been found for the ILs with the most unsymmetrical anions

Table 2. Thermal properties of the K^+ and $[EMIm]^+$ salts.^[a]

anion	K^+ salt ^[b]		$[EMIm]^+$ salt ^[c]			
	T_{mp} [°C]	T_{dec} [°C]	T_{fp} [°C]	T_g [°C]	T_{mp} [°C]	T_{dec} [°C]
1a ^[d]	-	270	-72 ^[e]	-	-21	265
1b	-	200	-97 ^[e]	-123	-34	215
1c	-	300	-72	-	-30	270
1d	200	320	-53	-	-7	330
2a ^[f]	-	270	-54	-	1	290 ^[g]
2b	-	260	-86	-	-57	260 ^[g]
2c	-	310	-74 ^[e]	-110	-21	330
2d	190	350	-57	-	-7	375
3a	-	296 ^[h]	-	-	8 ^[i]	304 ^[i]
3b	138	180	-86 ^[e]	-112	-53	265 ^[g]
4a	-	300 ^[h]	-	-	-4 ^[i]	277 ^[i]
4b	190	220	-67 ^[e]	-	-36	260 ^[g]
$[BF_4]^-$	570 ^[j]	-	-60 ^[j]	-93 ^[j]	15 ^[j]	420 ^[j]
TCB	430 ^[k]	510 ^[k]	-55	-	8 ^[l]	420
I	365 ^[m,n]	370 ^[n]	n.o. ^[o]	n.o.	n.o.	n.o.
II	-	320 ^[p]	-	-	125 ^[q]	325

[a] All temperatures are onset values (rounded down for the decomposition temperature (T_{dec}), except for literature values); T_{fp} = freezing point; T_{mp} = melting point; T_g = glass transition temperature. [b] T_{mp} and T_{dec} determined by DSC and confirmed visually. [c] Phase transition temperatures determined by DSC; T_{dec} determined by TGA. [d] Literature data for $[EMIm]1a$: T_g = -117 °C; T_{fp} = -80 °C; T_{mp} = -20 °C; T_{dec} = 246 °C.^[35] [e] Only part of the IL crystallizes at the given temperature upon cooling, the remainder crystallizes upon heating at approximately the same temperature. [f] Literature data for $K2a$: T_{dec} = 287 °C;^[39] for $[EMIm]2a$: T_{mp} = 1 °C; T_{dec} = 305 °C.^[35] [g] Onset of a continuous loss of mass. [h] Ref. [39]. [i] Ref. [35]. [j] Ref. [60]. [k] Ref. [5]. [l] Ref. [1]. [m] Melts under decomposition. [n] Ref. [44]. [o] n.o. = not observed. [p] Ref. [17]. [q] Phase transition at 81 °C.

**Figure 4.** a) Melting point (T_{mp}), b) freezing point (T_{fp}) and c) decomposition temperature (T_{dec}) of $[EMIm][C_nF_{2n+1}BF_{3-x}(CN)_x]$ ($n = 1-4$; $x = 0-3$).

with minima for $[EMIm]2b$ and $[EMIm]3b$ with -57 and -53 °C, respectively (Figure 4a). Noticeably, the length of the perfluoroalkyl chain has different effects on T_{mp} for $[EMIm][R^F BF_3]$ and $[EMIm][R^F BF_2(CN)]$ as evident from Figure 4a. The $EMIm$ -ILs show supercooling behaviour with freezing points (T_{fp}) of up to -97 °C for $[EMIm]1b$ (Table 2, Figure 4b).

The salts $[EMIm][R^F BF_{3-x}(CN)_x]$ ($x = 0-3$) are thermally very robust as shown by their decomposition temperatures (Table 2, Figure 4c). As a consequence of the low melting points and the high thermal stabilities, the new RTILs based on mono(perfluoroalkyl)cyanofluoroborate anions provide large liquid ranges. The $EMIm$ -monocyanoborates $[EMIm][R^F BF_2(CN)]$ possess the lowest thermal stabilities in the series and the stability increases with increasing number of cyano groups. Thus, the perfluoroalkyltricyanoborates are the most stable ILs and their stability exceeds those of the respective perfluoroalkyltrifluoroborates, as well. Decomposition of the mixed perfluoroalkylcyanofluoroborates starts with dismutation of the cyano and fluorine substituents at boron. E.g. a sample of $[EMIm]2b$ was found to slowly dismutate to give $[EMIm]2a$ and $[EMIm]2c$ at 245 °C, a value slightly below T_{dec} determined by TGA (260 °C). Related dismutation reactions have been described for cyanofluoroborates, earlier.^[5] The gaseous decomposition products of the thermogravimetric analyses were studied by IR spectroscopy and mass spectrometry. All $EMIm$ -cyanoborates studied herein decompose under evolution of HCN (IR). All fluoroborates as well as $[EMIm][R^F B(CN)_3]$ lose fluorine as indicated by mass spectrometry. The mass spectra of the gaseous decomposition products of the pentafluoroethylborates showed the formation of tetrafluoroethylene C_2F_4 . $CF_3CF=CF_2$ was found during the decomposition of $[EMIm]3b$. Furthermore, decomposition of $[EMIm]1a$ and $[EMIm]1b$ gave some tetrafluoroethylene, as well, but not the degradation of $[EMIm]1c$ and $[EMIm]1d$.

The thermal stabilities of $[EMIm][R^F BF_{3-x}(CN)_x]$ ($x = 1-3$) parallel the B-F and B-CN bond dissociation energies ΔH calculated for the gas phase, which correspond to the fluoride and cyanide ion affinities of the Lewis acids $R^F BF_{2-x}(CN)_x$ ($x = 0-2$) (Tables S10 and S11 in the Supporting Information). According to the calculated fluoride and cyanide ion affinities, the B-CN bond(s) is(are) weaker than the B-F bond(s) for all mixed mono(perfluoroalkyl)cyanofluoroborate anions. Furthermore, loss of F^- at the α -carbon atom under formation of a di- or a monofluorocarbene borane complex, which is well documented for trifluoromethyl- and pentafluoroethylborate anions,^[5b] is thermodynamically the least favoured decomposition pathway for the borate anions.

The $EMIm$ -trifluoromethylborates are less stable than $[EMIm]^+$ salts of the pentafluoroethylborate anions with the same F/CN substitution scheme (Table 2, Figure 4c). The small change in T_{dec} of the $[EMIm]^+$ salts of **2b**, **3b** and **4b** shows that the influence of longer perfluoroalkyl chains is negligible. The instability of CF_3 -substituted borates compared to borates with longer perfluoroalkyl chains is rationalized by the F^- affinity of the corresponding fluorocarbene complexes of boron: difluorocarbene complexes are easier formed than monofluorocarbene complexes such as $CF_3CFB(CN)_3$ (Table S11 in the Supporting Information).

$K[R^F BF_{3-x}(CN)_x]$ ($x = 0-2$). The trends in thermal stability of the potassium salts $K[R^F BF_{3-x}(CN)_x]$ ($x = 0-2$) are similar to the ones discussed for the $EMIm$ -ILs (Table 2). The low stabilities of **K3b** and **K4b** are two exceptions. **K3b** and **K4b** decompose at

Table 3. Physical and electrochemical properties^[a] of [EMIm][R^FBF_{3-x}(CN)_x] (x = 0–3; R^F = perfluoroalkyl), [EMIm][BF₄], and [EMIm][B(CN)₄] ([EMIm]TCB) at 20 °C (values in italics: 25 °C).

anion	η [mPa·s]	ρ [g·cm ⁻³]	c [mol·L ⁻¹]	D^+ [10 ⁻¹¹ ·m ² ·s ⁻¹]	D^- [10 ⁻¹¹ ·m ² ·s ⁻¹]	σ [mS·cm ⁻¹]	Λ_{NMR} [cm ² ·S·mol ⁻¹]	Λ_{imp} [cm ² ·S·mol ⁻¹]	I [-]	E_{pc} [V]	E_{pa} [V]	ΔE [V]
1a	32.5	1.34	5.42	5.6	3.8	13.1	3.59	2.42	0.67	-2.5 ^[b]	2.1 ^[b]	4.6 ^[b]
1b	16.5	1.26	4.95	9.3	7.6	16.0	6.42	3.23	0.50	-2.5	2.6	5.1
1c	14.0	1.20	4.58	10.0	8.4	17.6	7.01	3.84	0.55	-2.5	2.3	4.8
1d	17.8	1.15	4.27	7.7	6.3	11.5	5.34	2.69	0.50	-2.4	2.4	4.8
2a	32.2	1.42	4.75	5.6	3.5	10.4	3.47	2.19	0.63	-2.5 ^[b]	2.1 ^[b]	4.6 ^[b]
2b	17.6	1.34	4.39	8.8	6.6	15.3	5.89	3.48	0.59	-2.6	3.2	5.8
2c	16.4	1.28	4.11	8.0	6.1	13.1	5.37	3.19	0.59	-2.4	2.4	4.8
2d	21.8	1.24	3.87	6.7	5.0	9.8	4.47	2.53	0.57	-2.4	2.1	4.5
3a ^{[c],[35]}	32	1.49	4.28	n.d. ^[d]	n.d.	8.6	n.d.	n.d.	n.d.	-2.6	2.1	4.7
3b	22.2	1.40	3.95	6.9	4.8	10.4	4.48	2.63	0.59	-2.5	2.8	5.3
4a ^{[c],[35]}	38	1.55	3.89	n.d.	n.d.	5.2	n.d.	n.d.	n.d.	-2.6	2.1	4.7
4b	30.8	1.46	3.59	5.1	3.4	7.1	3.26	1.98	0.61	-2.5	3.0	5.5
[BF ₄] ⁻ ^{[c],[35]}	42 ^[e]	1.28	6.46	n.d.	n.d.	13.6	n.d.	n.d.	n.d.	-2.5	2.0	4.5
TCB	21.8 ^[f]	1.04	4.60	6.3	5.4	12.1	4.47	2.64	0.59	-2.4 ^[1]	2.0 ^[1]	4.4 ^[1]

[a] Dynamic viscosity η ; density ρ ; concentration c ; diffusion coefficients of cations (D^+) and anions (D^-); specific conductivity σ measured via impedance spectroscopy; molar conductivities calcd. by $\Lambda_{\text{NMR}} = (D^+ + D^-) \cdot N_A \cdot e^2 \cdot k^{-1} \cdot T^{-1}$ and $\Lambda_{\text{imp}} = \sigma \cdot M \cdot \rho^{-1}$; ionicity $I = \Lambda_{\text{imp}} \cdot \Lambda_{\text{NMR}}^{-1}$; cathodic and anodic limits E_c and E_a ; electrochemical window $\Delta E = E_{\text{pa}} - E_{\text{pc}}$. [b] Data reported earlier: [EMIm]1a: $E_{\text{pc}} = -2.49$, $E_{\text{pa}} = 2.14$, $\Delta E = 4.63$ V; [EMIm]2a: $E_{\text{pc}} = -2.50$, $E_{\text{pa}} = 2.15$, $\Delta E = 4.65$ V. [c] Published data for: viscosity, density and conductivity at 25 °C; for cyclic voltammetry experiments no temperature was given.^[35] [d] n.d. = not determined. [e] 67 mPa·s at 20 °C.^[1] [f] The viscosity differs slightly from a value published, earlier ($\eta = 22.2$ mPa·s),^[1] which is due to the different methods employed.

180 and 220 °C whereas **K2b** is stable up to 260 °C. **K3b** and **K4b**, which are both liquids at these temperatures, are prone to dismutation more easily, which is evident from the DSC curves. **K2b** does not melt. So, dismutation of **K2b** is slow and it takes several hours until significant amounts were converted into other borates such as **K2a** and **K2c**.

The decomposition temperatures of the perfluoroalkyltricyanoborates **K1d** and **K2d** of 320 and 350 °C, respectively, are similar to T_{dec} of K[(CF₃)₃B(CN)] (370 °C)^[44] and K[B(CF₃)₄] (320 °C)^[17] but lower than T_{dec} reported for K[B(CN)₄] (510 °C).^[5] Furthermore, **K1d** and **K2d** are the sole potassium trifluoromethyl- and pentafluoroethylcyanoborates that melt (200 and 190 °C, respectively) before decomposition occurs.

Electrochemical stabilities of EMIm-ILs

The electrochemical stability of the neat EMIm-ILs was assessed by cyclic voltammetry at 20 °C. The cathodic (E_{pc}) and anodic limits (E_{pa}) and the electrochemical windows are listed in Table 3 and the respective voltammograms are shown in Figure S4 in the Supporting Information. The cathodic limit of all [EMIm]⁺ salts is similar with approximately -2.4 to -2.6 V and it is determined by the stability of the [EMIm]⁺ cation. In contrast, the anodic limit is strongly dependent on the borate anion and therefore the electrochemical windows differ. [EMIm][R^FBF₂(CN)] provide the largest electrochemical windows (>5 V) with a maximum of 5.8 V for [EMIm]2b. The mono(perfluoroalkyl)dicyanofluoroborates [EMIm][R^FBF(CN)₂] are electrochemically very stable, too, but the values (~4.8 V) are significantly smaller than the ones of [EMIm][R^FBF₂(CN)]. The lowest electrochemical stability was found for the mono(perfluoroalkyl)trifluoro- and -tricyanoborates although their stability is still high. The influence of the length of the perfluoroalkyl chain is small, which is in agreement to an earlier report on EMIm-ILs with the [R^FBF₃]⁻ anions.^[35] The biggest deviation is found for [EMIm]1b and [EMIm]2b with 5.1 and 5.8 V, respectively. The electrochemical windows of the [EMIm]⁺ salts of the anions [R^FB(CN)₃]⁻ are similar to the stabilities reported for [EMIm][R^FBF₃],^[35] [EMIm][BF₄]^[35] and [EMIm]TCB.^[1]

Viscosities, self-diffusivities and conductivities of EMIm-ILs

Dynamic viscosities. The [EMIm]⁺ salts based on the new mono(perfluoroalkyl)cyanofluoroborate anions [C_nF_{2n+1}BF_{3-x}(CN)_x]⁻ ($n = 1-4$; $x = 0-3$) are low-viscosity RTILs (Table 3, Figures 5 and 6). [EMIm][CF₃BF(CN)₂] ($\eta = 14.0$ mPa·s) has the lowest dynamic viscosity at 20 °C of the new [EMIm]⁺ salts presented, herein, which is much lower than those of [EMIm][BF₄] (67 mPa·s) and [EMIm]TCB (21.8 mPa·s) and close to the one of [EMIm]MFB (12.6 mPa·s).^[1] The viscosity strongly decreases with increasing temperature and their differences become smaller (Figure 5). The decrease in viscosity with higher temperature is less pronounced for the EMIm-perfluoroalkylcyano(fluoro)borates than for [EMIm]TCB.

The unsymmetrical anions of the type [C_nF_{2n+1}BF₂(CN)]⁻ and [C_nF_{2n+1}BF(CN)₂]⁻ result in ILs with the lowest viscosities in the respective series of perfluoroalkylborates. This effect is similar to the one found for the melting and freezing points (Table 2, Figure 4). In addition to this symmetry-related effect, an increasing number of cyano groups has a beneficial influence with regard to lower viscosities. This is rationalized by the more efficient charge delocalization due to the strong electron-withdrawing cyano groups.^[1] So, lower viscosities are observed (i) for [EMIm][C_nF_{2n+1}B(CN)₃] compared to the respective [EMIm]-[C_nF_{2n+1}BF₃] and (ii) for [EMIm][C_nF_{2n+1}BF(CN)₂] compared to the corresponding [EMIm][C_nF_{2n+1}BF₂(CN)]. The interplay of symmetry and content of CN groups makes [EMIm]1c and [EMIm]2c to the ILs having the lowest viscosity in the series of trifluoromethyl- and pentafluoroethylborates, respectively.

The viscosity increases with longer perfluoroalkyl chains as exemplified by the series [EMIm][C_nF_{2n+1}BF₂(CN)] ($n = 1-4$, **1b-4b**; Figure 6). This trend basically parallels the one reported for the corresponding trifluoroborates, earlier, with one exception, the viscosity of [EMIm]1a (32.5 mPa·s) and [EMIm]2a (32.2 mPa·s) that are almost the same (Figure 6).^[35] The difference between the trifluoromethyl- and the related pentafluoroethylborate is small, in general, but it increases with an increasing number of cyano groups (Figure 6). The higher viscosities for anions with longer perfluoroalkyl chains may be explained by

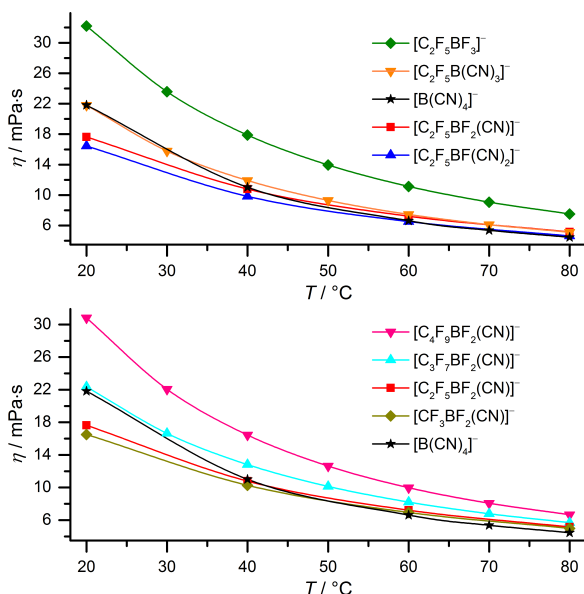


Figure 5. Temperature dependence of the dynamic viscosity (η) of [EMIm] $[\text{C}_n\text{F}_{2n+1}\text{BF}_{3-x}(\text{CN})_x]$ ($n = 1-4$; $x = 0-3$) and [EMIm]TCB.

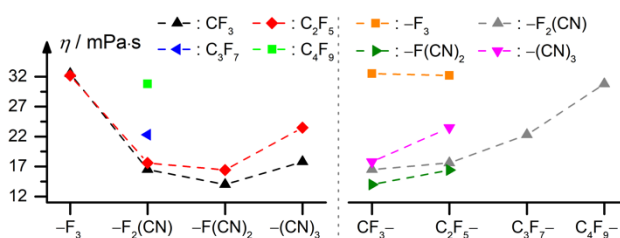


Figure 6. Dynamic viscosity (η) of [EMIm] $[\text{C}_n\text{F}_{2n+1}\text{BF}_{3-x}(\text{CN})_x]$ ($n = 1-4$; $x = 0-3$) at 20 °C.

stronger van der Waals interactions^[35] and the higher mass of the anions.^[61] The exception discussed for [EMIm]1a and [EMIm]2a reflects the strong gain in charge delocalization of a C_2F_5 versus a CF_3 group. This effect becomes less important the more CN groups are present at boron because of their efficient charge delocalization. This results in (i) significantly lower viscosities for [EMIm] $[\text{CF}_3\text{BF}_{3-x}(\text{CN})_x]$ compared to [EMIm] $[\text{C}_2\text{F}_5\text{BF}_{3-x}(\text{CN})_x]$ ($x = 1-3$) and (ii) a steady increase in $\Delta[\eta([\text{EMIm}][\text{C}_2\text{F}_5\text{BF}_{3-x}(\text{CN})_x] - \eta([\text{EMIm}][\text{CF}_3\text{BF}_{3-x}(\text{CN})_x])]$ with increasing x .

Densities. The densities of the EMIm-ILs based on the anions $[\text{C}_n\text{F}_{2n+1}\text{BF}_{3-x}(\text{CN})_x]^-$ ($n = 1-4$; $x = 0-3$) are higher than the density of [EMIm]MFB ($1.07 \text{ g}\cdot\text{cm}^{-3}$). The density increases with longer perfluoroalkyl chains and it decreases with increasing number of cyano groups (Table 3). Analogous trends have been reported for [EMIm] $[\text{C}_n\text{F}_{2n+1}\text{BF}_3]$ ($n = 1-4$)^[35] and [EMIm] $[\text{BF}_{4-x}(\text{CN})_x]$ ($x = 0-4$).^[1]

Conductivities. The EMIm-ILs with the mixed perfluoroalkyl-cyanofluoroborate anions $[\text{C}_n\text{F}_{2n+1}\text{BF}_{3-x}(\text{CN})_x]^-$ ($x = 1, 2$; $n = 1, 2$) exhibit extraordinary high specific conductivities (σ) of up to $17.6 \text{ mS}\cdot\text{cm}^{-1}$ for [EMIm]1c at 20 °C (Table 3). These conductivities are much higher than σ of EMIm-perfluoroalkyltrifluoroborates.^[35] Furthermore, specific conductivities of non-protic ILs are usually smaller than $10 \text{ mS}\cdot\text{cm}^{-1}$ at 20 °C,^[62] e.g. $9.6 \text{ mS}\cdot\text{cm}^{-1}$ for [EMIm] (CF_3CO_2) .^[63] In addition to the impedance

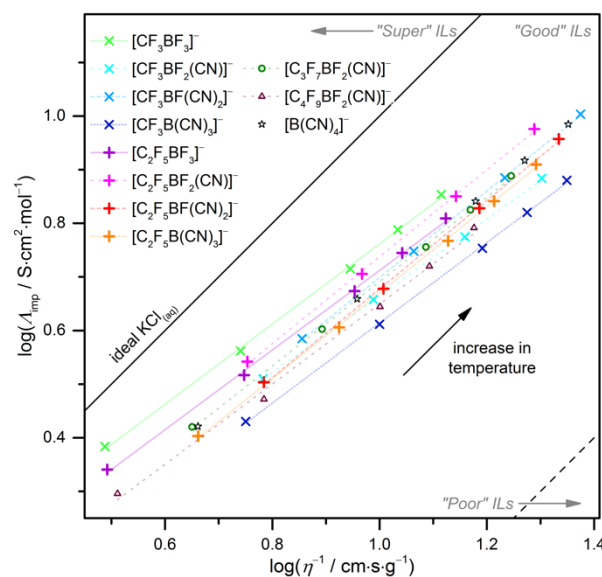


Figure 7. Walden plot for [EMIm] $[\text{C}_n\text{F}_{2n+1}\text{BF}_{3-x}(\text{CN})_x]$ ($x = 0-3$) and [EMIm]TCB

measurements performed at 20 °C, the specific conductivities were studied at 40, 60, and 80 °C and for higher temperatures higher conductivities were observed (Table S1 in the Supporting Information).

The specific conductivity of an ionic liquid is governed by its dynamic viscosity and density as well as the molecular mass and size of the ions.^[63] The density of the IL and the molecular mass and size of ions, which determine the concentration (c), are a measure for the number of carrier ions. On the contrary, the dynamic viscosity describes the particle mobility. A combination of high concentration of the carrier ions and low viscosity results in a high specific conductivity. So, it is rationalized that longer perfluoroalkyl chains result in lower specific conductivities for each series of EMIm-ILs. The successive exchange of fluorine against CN is accompanied by decreasing concentrations (c) and dynamic viscosities, which both have opposing effects on σ . Since the EMIm-ILs based on the mixed perfluoroalkyl-cyanofluoroborate anions $[\text{C}_n\text{F}_{2n+1}\text{BF}_{3-x}(\text{CN})_x]^-$ ($x = 1, 2$; $n = 1, 2$) have very low viscosities but still high concentrations (c), their specific conductivities are extraordinary high (Table 3). The respective [EMIm] $[\text{C}_n\text{F}_{2n+1}\text{B}(\text{CN})_3]$ have higher viscosities and lower densities than the EMIm-ILs with the less symmetrical anions $[\text{C}_n\text{F}_{2n+1}\text{BF}_{3-x}(\text{CN})_x]^-$ ($x = 1, 2$; $n = 1, 2$). This explains the significantly lower specific conductivities of [EMIm] $[\text{C}_n\text{F}_{2n+1}\text{B}(\text{CN})_3]$. This gives even lower σ for [EMIm] $[\text{C}_n\text{F}_{2n+1}\text{B}(\text{CN})_3]$ compared to [EMIm] $[\text{C}_n\text{F}_{2n+1}\text{BF}_3]$.

In contrast to the specific conductivity, the molar conductivity Λ_{imp} mostly depends on the dynamic viscosity. So, [EMIm] $[\text{C}_n\text{F}_{2n+1}\text{B}(\text{CN})_3]$ reveal higher Λ_{imp} than the respective [EMIm] $[\text{C}_n\text{F}_{2n+1}\text{BF}_3]$ (Table 3). The other dependencies found for Λ_{imp} are basically the same as those discussed for σ . The Walden plot depicted in Figure 7 shows that the EMIm-ILs based on the anions $[\text{C}_n\text{F}_{2n+1}\text{BF}_{3-x}(\text{CN})_x]^-$ ($x = 0-3$) and on the TCB anion can be classified as good ILs.^[64]

Self-diffusion coefficients were extracted for the anions (D^-) and cations (D^+) from diffusion-ordered spectroscopy (DOSY) NMR measurements performed at 20, 40 and 60 °C (Table 3 and S1 in the Supporting Information). The diffusion coefficients of [EMIm] $[\text{C}_n\text{F}_{2n+1}\text{BF}_{3-x}(\text{CN})_x]$ were derived from ^1H (D^+) and ^{19}F

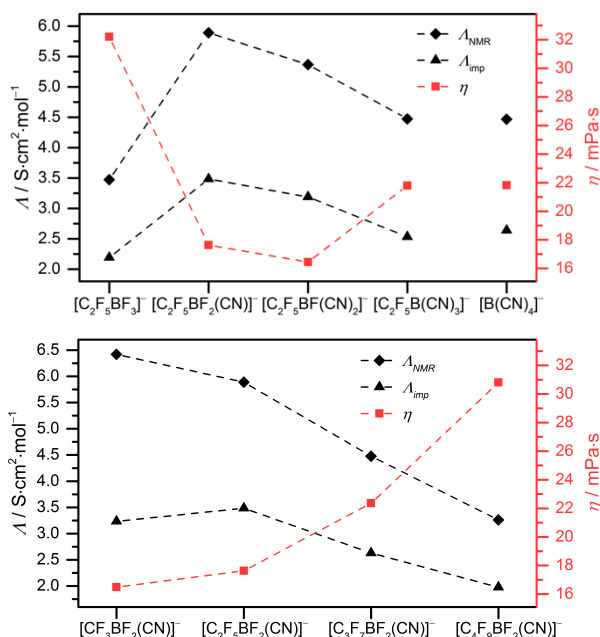


Figure 8. Dynamic viscosities (η) and molar conductivities (Λ) as a function of the number of CN groups of the perfluoroalkylborate anions and the TCB anion (top) and of the length of the perfluoroalkyl group of the mono(perfluoroalkyl)difluorocyanoborate anions (bottom), respectively (20 °C).

DOSY NMR experiments (D^-). For selected EMIm-ILs ¹¹B DOSY NMR studies were performed, as well, that gave identical D^- . The diffusion coefficients of [EMIm]TCB were determined by ¹H (D^+), ¹¹B (D^-) and ¹³C DOSY NMR measurements (D^+ and D^-). D^+ and D^- extracted from the ¹³C DOSY NMR study were basically identical to D^+ and D^- derived from ¹H and ¹¹B experiments, respectively. For all EMIm-ILs, the diffusion coefficient of the cation is slightly larger than D^- of the anion.

The molar conductivity Λ_{NMR} was calculated from the diffusion coefficients D^+ and D^- using the Nernst-Einstein equation (Table 3). Λ_{NMR} is much higher than Λ_{imp} for all ILs and both molar conductivities Λ_{NMR} and Λ_{imp} follow basically the same trends (Figure 8). For example, the mixed EMIm-perfluoroalkylcyanofluoroborates [EMIm][C₂F₅BF_{3-x}(CN)_x] ($x = 1$ (**2b**), 2 (**2c**)) have higher Λ_{NMR} compared to [EMIm]**2a** and [EMIm]**2d**. The ratio of Λ_{imp} to Λ_{NMR} that is termed ionicity (I) can be regarded as a measure for the ion-pairing of an IL (Table 3, Figure S2).^[65] The ionicities are in the range of 0.50 to 0.67 for the EMIm-ILs discussed herein and no trend concerning I is evident.

Temperature-dependent fitting of η and σ . The experimental dynamic viscosities measured at different temperatures were fitted with the Vogel-Fulcher-Tammann (VFT) ansatz (Eq. 1 in the Supporting Information), which is often used to describe the thermal behaviour of glass-forming liquids.^[66] The fits give very good results for all RTILs ($R^2 \geq 99.99\%$) and the fit parameters are given in Table S2 and the fitted curves are shown in Figure S5 in the Supporting Information.

The conductivities were fitted using a VFT,^[66] Arrhenius,^[67] and Litovitz^[68] ansatz (Eq. 2–4 in the Supporting Information). All three equations were found to be well suited for the description of the temperature dependence of the specific conductivities ($R^2 \geq 99.6\%$). The standard deviation of the Arrhenius fitting increases with increasing number of CN groups bonded to boron. Hence, relatively large deviations were found for the tricyano-

borates and the largest for [EMIm]TCB that has the maximum number of four cyano groups at boron. For the VFT and Litovitz fittings the opposite trend was found, although the absolute standard deviations are very small for both models. An Arrhenius behaviour is indicative for non-associating electrolytes,^[67] whereas Litovitz behaviour points towards associating electrolytes.^[68] Hence, the present results indicate a slight change in the behaviour from non-associating to more associating electrolytes with an increasing number of cyano groups. The good fitting according to the VFT approach is in accordance to the observation of glass transitions for some of the RTILs by DSC (Table 2).

Dye-sensitized solar cells (DSSCs) with EMIm-cyanoborate-ILs

Selected EMIm-ILs with the new perfluoroalkylcyano(fluoro)borate anions were employed as component of the electrolyte of dye-sensitized solar cells (DSSCs, Grätzel cells^[69]).^[50] [EMIm]TCB was introduced as a non-volatile component of electrolytes for DSSCs, earlier,^[8] and it was employed in the same setup as the new RTILs as a reference.^[50] According to the DSSC data collected in Table 4, the four EMIm-ILs with mixed perfluoroalkylcyanofluoroborate anions **1b**, **1c**, **2b** and **2c** result in higher efficiencies than [EMIm]TCB. The highest efficiency was achieved with [EMIm][CF₃BF(CN)₂] that has the lowest viscosity within the investigated series of ILs. In general, the efficiency decreases with increasing viscosity, which explains the inferior performance of the cell that contained [EMIm]TCB.

Table 4. DSSC efficiencies with electrolytes based on EMIm-cyanoborate RTILs at 25 °C^[a] and dynamic viscosities of the neat RTIL at 20 °C.^[50]

salt	DSSC efficiency ^[a]	η (20 °C)
	(25 °C, AM ^[b] 1.5)	[mPa·s]
[EMIm] 1b	5.8 ± 0.8%	16.5
[EMIm] 1c	6.0 ± 0.8%	14.0
[EMIm] 2b	5.5 ± 0.3%	17.6
[EMIm] 2c	5.4 ± 0.3%	16.4
[EMIm]TCB	5.2 ± 0.5%	22.2

[a] Composition of the electrolyte (molar ratio): 36 [MMIm] (MMIm = 1,3-dimethylimidazolium), 36 [EMIm], 5 I₂, 48 [EMIm][R^FBF_{3-x}(CN)_x] or [EMIm]TCB, 2 [C(NH₂)₃]SCN, 10 *N*-butylbenzimidazole. [b] AM = air mass coefficient.

Summary and Conclusions

Potassium salts of perfluoroalkyltricyanoborate and mono(perfluoroalkyl)cyanofluoroborate anions have become available in high purity and on a large scale via different synthetic approaches. These potassium salts have been found to be well-suited for metathesis reactions giving, e.g. [EMIm]⁺ salts that are room-temperature ionic liquids (RTILs). These RTILs possess very low viscosities, extraordinary high specific conductivities and low melting and freezing points. The highest conductivities, lowest viscosities and melting as well as freezing points were found for the most unsymmetrical borate anions [C_nF_{2n+1}BF_{3-x}(CN)_x]⁻ ($n = x = 1, 2$). Especially the salts of the anions [R^FBF(CN)₂]⁻ and [R^FB(CN)₃]⁻ reveal very high thermal stabilities and they are chemically and electrochemically very robust. In summary, EMIm-ILs based on the mono(perfluoroalkyl)dicyanofluoroborate anions [CF₃BF(CN)₂]⁻ (**1c**) and [C₂F₅BF(CN)₂]⁻ (**2c**) provide a desirable combination of properties required for ILs

used for example in electrochemical devices. A first demonstration is given by their application in dye-sensitized solar cells (DSSCs, Grätzel cells^[69]) and it has to be expected that others will follow. In addition, with the synthesis of first lanthanide frameworks with the $[\text{C}_2\text{F}_5\text{B}(\text{CN})_3]^-$ anion, the value of the mono-(perfluoroalkyl)cyanoborate anions for coordination chemistry and luminescent materials was already demonstrated.^[48]

Experimental Section

General: Reactions involving air-sensitive compounds were performed either in 100 or 250 mL round bottom flasks or in 20 or 60 mL glass tubes equipped with valves with PTFE stems (Young, London) under argon using standard Schlenk line techniques. For reactions under high pressure (>5 bar) an autoclave BR-300 (Co. Berghof, 72800 Enningen, Germany; capacity 350 mL) equipped with an anchor agitator, an internal temperature control unit as well as a manometer was used. Some reactions were performed in glass fingers equipped with stems with PTFE valves under microwave irradiation (CEM Discover S-Klasse Plus (SP)). ¹¹B, ¹⁹F, and ¹³C NMR spectra were recorded at 25 °C in (CD₃)₂CO on a Bruker Avance I 500 spectrometer. ¹³C{¹H} NMR spectra were recorded on a Bruker Avance III HD 300 spectrometer. For the ¹³C NMR spectra concentrated solutions (100–500 mg in 0.7 mL (CD₃)₂CO) were used. The concentrated samples were diluted to ensure small line widths in the ¹¹B and ¹⁹F spectra (30–100 mg in 0.7 mL (CD₃)₂CO). The ¹³C{¹⁹F} NMR spectra were recorded on the Bruker Avance I 500 spectrometer equipped with a Prodigy-Cryoprobe using a simple zgig pulse sequence. The broadband fluorine decoupling was achieved with the adiabatic decoupling scheme p5m4sp180.2 using a smoothed chirp shape pulse with 500 μs pulse length to ensure a decoupling bandwidth of 85 kHz or 180 ppm for ¹⁹F. The NMR signals were referenced against TMS (¹H and ¹³C), BF₃·OEt₂ in CDCl₃ with $\delta(^{11}\text{B}) = 32.083974\%$, and CFC₃ with $\delta(^{19}\text{F}) = 94.094011\%$ as external standards.^[70] ¹H and ¹³C chemical shifts were calibrated against the residual solvent signal and the solvent signal, respectively ($\delta(^1\text{H})$: (CD₂H)(CD₃)CO 2.05 ppm; $\delta(^{13}\text{C})$: (CD₃)₂CO 29.84 and 206.26 ppm).^[71] IR spectra were recorded at room temperature on an Excalibur FTS 3500 spectrometer (Digilab, Germany), on a Nicolet 380 spectrometer or on a Bruker Alpha spectrometer. IR spectra were measured in the attenuated total reflection (ATR) mode in the region of 4000–530 cm⁻¹ with an apodized resolution of 4 cm⁻¹. Raman spectra were recorded using the 1064 nm excitation line of a Nd/YAG laser on crystalline samples contained in melting point capillaries in the region of 3500–80 cm⁻¹ at room temperature either on an Excalibur FTS 3500 spectrometer (Digilab, Germany) with an apodized resolution of 4 cm⁻¹ or on a Bruker IFS-120 spectrometer with an apodized resolution of 1 cm⁻¹, respectively. Matrix-assisted laser desorption/ionization (MALDI) mass spectra in the negative-ion mode were recorded on a Bruker Ultraflex TOF spectrometer. DSC measurements were performed with a Netzsch DSC 204F1 Phoenix in the temperature range of 25 to -180 °C with a cooling and heating rate of 5 K·min⁻¹ and DTA measurements were performed with a Netzsch STA 449 C in the temperature range of 32 to 500 °C with a heating rate of 10 K·min⁻¹. The water content of the ILs was determined by Karl-Fischer titration using a 831 KF Coulometer (Metrohm). Viscosities were measured on samples with a minimum volume of 3.5 mL using a SVM 3000 Stabinger viscometer (Anton Paar, Austria). Elemental analyses (C, H, N) were performed either with a Euro EA3000 instrument (HEKA-Tech, Germany) or a Perkin-Elmer EA240 instrument.

Chemicals: All standard chemicals were obtained from commercial sources. Solvents were dried according to standard protocols^[72] and stored in flasks equipped with valves with PTFE stems (Young, London) over molecular sieves (4 Å) under an argon atmosphere. $[\text{K}(\text{C}_n\text{F}_{2n+1}\text{BF}_3)]$ ($n = 1-4$) were obtained from $M[\text{C}_n\text{F}_{2n+1}\text{B}(\text{OMe})_3]$ ($M = \text{Li}, \text{K}; n = 1-4$) and anhydrous HF as reported for $[\text{K}(\text{C}_2\text{F}_5\text{BF}_3)]$.^[73] $M[\text{C}_n\text{F}_{2n+1}\text{B}(\text{OMe})_3]$ was synthesized according to known procedures starting from $\text{B}(\text{OMe})_3$ with CF_3SiMe_3 ,^[74] $n\text{BuLi}$, and $\text{C}_2\text{F}_5\text{H}$,^[41] $t\text{BuLi}$ and $\text{C}_3\text{F}_7\text{H}$,^[33] or Mg and

C_4F_9 ,^[43] respectively. $[\text{K}(\text{B}(\text{CF}_3)_4)]$ was synthesized as described earlier.^[16,17] Me_3SiCN and Et_3SiCN were synthesized according to a modified literature procedure reported for Me_3SiCN .^[75]

Syntheses of Potassium Salts

$[\text{K}(\text{C}_2\text{F}_5\text{BF}_2(\text{CN}))]$ (K1b): K1a (3.0 g, 17.0 mmol) was stirred with Me_3SiCN (6.0 mL, 45.0 mmol) at room temperature for 20 hrs. All volatiles were removed under reduced pressure and most of the excess of the Me_3SiCN (3.0 mL, 22.5 mmol) was recovered by fractional distillation. The crude product was taken up into THF (3 mL) and addition of CH_2Cl_2 (150 mL) resulted in K1b as a colourless solid, which was isolated by filtration and subsequent drying in a vacuum. Yield: 3.00 g (16.4 mmol, 96%). ¹³C NMR: $\delta = 130.0$ (qt, 1C, $^1J(^{19}\text{F}, ^{13}\text{C}) = 308.1$ Hz, $^2J(^{19}\text{F}, ^{13}\text{C}) = 43.3$ Hz, CF₃), 129.8 ppm (t, 1C, $^2J(^{19}\text{F}, ^{13}\text{C}) = 48.7$ Hz, CN). ¹¹B NMR: $\delta = -3.8$ ppm (tq, 1B, $^1J(^{19}\text{F}, ^{11}\text{B}) = 48.8$ Hz, $^2J(^{19}\text{F}, ^{11}\text{B}) = 34.6$ Hz). ¹⁹F NMR: $\delta = -77.5$ (qt, 3F, $^2J(^{19}\text{F}, ^{11}\text{B}) = 34.6$ Hz, $^3J(^{19}\text{F}, ^{19}\text{F}) = 1.9$ Hz, CF₃), -169.2 ppm (qq, 2F, $^1J(^{19}\text{F}, ^{11}\text{B}) = 48.8$ Hz, $^3J(^{19}\text{F}, ^{19}\text{F}) = 1.9$ Hz, BF₂). Raman: 2233, 2226 cm⁻¹ ($\nu(\text{C}\equiv\text{N})$). MALDI-MS: m/z (isotopic abundance) calcd. for **1b** ($[\text{C}_2\text{BF}_5\text{N}]^-$): 144(100), 143(25), 145(2); found: 144(100), 143(27), 145(5). Anal. calcd. for Elemental analysis calcd (%) for C₂BF₅KN: C 13.13, N 7.66; found: C 13.29, N 7.62.

$[\text{K}(\text{C}_2\text{F}_5\text{BF}_2(\text{CN}))]$ (K1b) with Me_3SiCl : K1a (6.00 g, 34.1 mmol) was suspended in Me_3SiCN (60 mL, 450 mmol). Upon addition of Me_3SiCl (4.0 mL, 31 mmol) the suspension immediately turned into a clear solution that was stirred for 10 minutes. All volatiles were removed under reduced pressure and most of the excess Me_3SiCN was recovered by fractional distillation. The slightly coloured residue was dissolved in water and several drops of aqueous H₂O₂ (30% v/v) and K₂CO₃ (1 g) were added. After stirring for 5 hrs, the mixture was concentrated under reduced pressure until K₂CO₃ began to precipitate. The mixture was extracted with THF (3 × 50 mL), the combined organic layers were dried with K₂CO₃, filtered, and concentrated to a volume of 10 mL. CH_2Cl_2 (100 mL) was added and a colourless precipitate formed that was collected by filtration and dried in a vacuum. Yield: 5.80 g (31.7 mmol, 93%).

$[\text{K}(\text{C}_3\text{BF}_3(\text{CN})_2)]$ (K1c) using MW irradiation: Trimethylsilyl cyanide (17.1 mL, 127.5 mmol) and K1a (6.0 g, 34.1 mmol) were stirred at room temperature for 12 days to give K1b according to NMR spectroscopy. Most of the trimethylsilyl fluoride, which had formed in the course of the reaction, was removed under reduced pressure. The reaction mixture was irradiated using a microwave oven (CEM Discover; 200 W, $T_{\text{max}} = 90$ °C) for 20 minutes. All volatiles were removed under reduced pressure and most of the remaining Me_3SiCN (6.3 mL, 47.2 mmol) was recovered by fractional distillation. The solid brownish residue was taken up into aqueous H₂O₂ (50 mL, 30% v/v) and was stirred for 1 hr. The pH of the solution was adjusted to 1 by the addition of conc. hydrochloric acid. Tri-*n*-propylamine (7.0 mL, 36.8 mmol) was added while stirring and the crude $[\text{nPr}_3\text{NH}]\text{1c}$ was extracted with CH_2Cl_2 (3 × 50 mL). The combined organic fractions were dried with MgSO₄, filtered and a solution of KOH in water (6 g, 30 mL) was added. The organic layer was removed and extracted with an aqueous solution of KOH (6 g, 30 mL). The collected aqueous KOH solutions were extracted with THF (3 × 50 mL). The three THF phases were combined, dried with K₂CO₃ and filtered. The volume of the THF solution was reduced until a viscous solution was obtained. Pure K1c precipitated upon addition of CH_2Cl_2 (150 mL). The salt was filtered off and dried in a vacuum. Yield: 5.0 g (26.3 mmol, 77%). ¹³C NMR: $\delta = 130.1$ (qd, 1C, $^1J(^{19}\text{F}, ^{13}\text{C}) = 305.4$ Hz, $^2J(^{19}\text{F}, ^{13}\text{C}) = 31.8$ Hz, CF₃), 127.8 ppm (dq, 2C, $^2J(^{19}\text{F}, ^{13}\text{C}) = 35.8$ Hz, $^3J(^{19}\text{F}, ^{13}\text{C}) \approx 2$ Hz, CN). ¹¹B NMR: $\delta = -12.8$ ppm (dq, 1B, $^1J(^{19}\text{F}, ^{11}\text{B}) = 49.1$ Hz, $^2J(^{19}\text{F}, ^{11}\text{B}) = 35.7$ Hz). ¹⁹F NMR: $\delta = -74.0$ (qd, 3F, $^2J(^{19}\text{F}, ^{11}\text{B}) = 35.7$ Hz, $^3J(^{19}\text{F}, ^{19}\text{F}) = 8.9$ Hz, CF₃), -219.9 ppm (qq, 1F, $^1J(^{19}\text{F}, ^{11}\text{B}) = 49.1$ Hz, $^3J(^{19}\text{F}, ^{19}\text{F}) = 8.9$ Hz, BF). Raman: 2228 cm⁻¹ ($\nu(\text{C}\equiv\text{N})$). MALDI-MS: m/z (isotopic abundance) calcd. for **1c** ($[\text{C}_3\text{BF}_4\text{N}_2]^-$): 151(100), 150(25), 152(4); found: 151(100), 150(24), 152(3). Elemental analysis calcd (%) for C₃BF₄KN₂: C 18.97, N 14.75; found: C 19.08, N 14.58

$[\text{K}(\text{C}_3\text{BF}_3(\text{CN})_2)]$ (K1c) with Me_3SiCl : K1c was prepared similar to K1b with Me_3SiCl starting from K1a (6.00 g, 34.1 mmol), Me_3SiCN (60 mL, 450 mmol), and Me_3SiCl (4.0 mL, 31 mmol). The reaction mixture was

stirred at 90 °C for 3 days and an off-white powder was obtained after work-up. Yield: 6.00 g (31.6 mmol, 93%).

K[CF₃B(CN)₃] (K1d) using MW irradiation. K1a (0.50 g, 2.8 mmol) and Me₃SiCN (10.0 mL, 74.9 mmol) were stirred at 100 °C for 2 hrs. The Me₃SiF was continuously allowed to evaporate from the reaction mixture. The closed reaction vessel was placed into a microwave oven and irradiated for 95 minutes (300 W, T_{max} = 120 °C). Subsequently, all volatiles were removed under reduced pressure and most of the excess Me₃SiCN (8.0 mL, 59.9 mmol) was recovered by fractional distillation. The solid residue was dissolved in aqueous H₂O₂ (5.0 mL, 30% v/v) and K₂CO₃ was added. The mixture was stirred for 1 hr and evaporated to dryness at a rotary evaporator. The solid remainder was extracted with ether (3×50 mL). The volume of the combined ethereal layers was reduced to 5 mL and colourless K1d precipitated upon addition of CH₂Cl₂ (100 mL). The solid was filtered off and dried in a vacuum. Yield: 0.53 g (2.7 mmol, 95%). ¹³C NMR: δ = 130.0 (q, 1C, ¹J(¹⁹F, ¹³C) = 301.7 Hz, CF₃), 123.6 ppm (q, 3C, ³J(¹⁹F, ¹³C) ≈ 3 Hz, CN). ¹¹B NMR: δ = -32.0 ppm (q, 1B, ²J(¹⁹F, ¹¹B) = 36.3 Hz). ¹⁹F NMR: δ = -66.4 ppm (q, 1F, ²J(¹⁹F, ¹¹B) = 36.3 Hz, CF₃). Raman: 2237, 2231 cm⁻¹ (ν(C≡N)). MALDI-MS: m/z (isotopic abundance) calcd. for 1d ([C₄BF₃N₃]⁻): 158(100), 157(25), 159(6); found: 158(100), 157(24), 159(5). Elemental analysis calcd (%) for C₄BF₃N₃: C 24.39, N 21.33; found: C 24.49, N 21.22.

K[CF₃B(CN)₃] (K1d) with Me₃SiCl in an autoclave: K1a (17.5 g, 99.5 mmol) was placed into an autoclave and Me₃SiCN (210 mL, 1.56 mol) and Me₃SiCl (15.0 mL, 119 mmol) were added. The reaction mixture was heated to 205 °C and stirred for 8 hrs, including the heating and cooling periods. The maximum pressure was approximately 14 bar. All volatiles were removed under reduced pressure and the black residue was dried in a vacuum overnight. The residue was dissolved in H₂O (30 mL), filtered through a plug of Celite, and treated with aqueous H₂O₂ (3×20 mL, 30% v/v) and K₂CO₃ (20 g). After stirring overnight, the mixture was concentrated under reduced pressure until K₂CO₃ began to precipitate. The mixture was extracted with THF (3×100 mL), the combined organic layers were dried with K₂CO₃, filtered, and concentrated to a volume of 30 mL. Slow addition of CH₂Cl₂ (300 mL) yielded two crops of (semi)solids. The first minor fraction was a black slime that was discarded. The second crop was an off-white solid that was collected by filtration and dried in a vacuum. Yield: 14.0 g (76.2 mmol, 77%).

K[CF₃B(CN)₃] (K1d) with Me₃SiCl: K1d was prepared similar to K1b with Me₃SiCl starting from K1a (3.00 g, 17.1 mmol), Me₃SiCN (10.0 mL, 112 mmol), and Me₃SiCl (2.0 mL, 15.7 mmol). The reaction mixture was stirred in a closed vessel at 130 °C for 2 hrs. Additional Me₃SiCN (10 mL, 74.9 mmol) and Me₃SiCl (1 mL, 7.86 mmol) were added and the reaction mixture was stirred for 3 weeks at 140 °C. The addition of CH₂Cl₂ (30 mL) resulted in a brownish slimy solid at the bottom of the flask that was removed from the colourless liquid. Colourless K1d precipitated during the addition of CH₂Cl₂ (150 mL) that was filtered off and dried in a vacuum. Yield: 1.90 g (9.65 mmol, 56%).

K[C₂F₅BF₂(CN)] (K2b): A mixture of K2a (15.8 g, 69.9 mmol) and trimethylsilyl cyanide (35.0 mL, 262.5 mmol) was stirred at 100 °C. The Me₃SiF that had formed was continuously distilled off during the reaction. All volatiles were removed under reduced pressure and most of the excess Me₃SiCN (21.3 mL, 159.9 mmol) was recovered by fractional distillation. The solid residue of the reaction mixture was dissolved in THF (5 mL). Neat, colourless K2b was precipitated by addition of CH₂Cl₂ (200 mL) that filtered off and dried in a vacuum. Yield: 15.8 g (67.8 mmol, 97%). ¹³C NMR: δ = 129.9 (t, 1C, ²J(¹⁹F, ¹³C) = 49.1 Hz, CN), 121.7 (qt, 1C, ¹J(¹⁹F, ¹³C) = 284.6 Hz, ²J(¹⁹F, ¹³C) = 31.8 Hz, CF₃), 117.4 ppm (ttq, 1C, ¹J(¹⁹F, ¹³C) = 258.8 Hz, ²J(¹⁹F, ¹³C) = 39.7 Hz, 36.5 Hz, CF₂). ¹¹B NMR: δ = -2.7 ppm (tt, 1B, ¹J(¹⁹F, ¹¹B) = 51.0 Hz, ²J(¹⁹F, ¹¹B) = 23.4 Hz). ¹⁹F NMR: δ = -83.2 (tt, 3F, ⁴J(¹⁹F, ¹⁹F) = 5.2 Hz, ³J(¹⁹F, ¹⁹F) = 0.9 Hz, CF₃), -136.3 (q, 2F, ²J(¹⁹F, ¹¹B) = 23.3 Hz, CF₂), -167.1 ppm (qq, 2F, ¹J(¹⁹F, ¹¹B) = 51.0 Hz, ⁴J(¹⁹F, ¹⁹F) ≈ 5 Hz, BF₂). Raman: 2233 cm⁻¹ (ν(C≡N)). MALDI-MS: m/z (isotopic abundance) calcd. for 2b ([C₃BF₂N]⁻): 194(100), 193(25), 195(4); found: 194(100), 193(28), 195(3). Elemental analysis calcd (%) for C₃BF₂N: C 15.47, H 0.00, N 6.01; found: C 15.39, H 0.55, N 6.01.

K[C₂F₅BF₂(CN)] (K2b) with Me₃SiCl: The procedure used for the preparation of K2b was similar to the one described for the synthesis of K1b in the presence of Me₃SiCl using K2a (15.0 g, 66.4 mmol), Me₃SiCN (100 mL, 0.75 mol), and Me₃SiCl (10 mL, 79 mmol). The crude product was a colourless oil. The crude product was dissolved in THF and the addition of CH₂Cl₂ resulted in K2b as a powder. The off-white hygroscopic powder was filtered off and stored under an inert atmosphere. Yield: 14.4 g (61.8 mmol, 93%).

K/Li[C₂F₅BF₂(CN)] (K/Li2b): K2a (100 mg, 0.44 mmol), LiCl (180 mg, 4.2 mmol), and KCN (260 mg, 3.99 mmol) were pestled and mixed inside a glove box and placed into a cylindrical reaction flask equipped with a glass valve and a PTFE stem (Young, London). The reaction mixture was heated to 180 °C for 20 hrs in a vacuum. According to the ¹¹B NMR spectroscopic analysis, the reaction mixture contained the following borate anions: [C₂F₅BF₂(CN)]⁻ (2b, 82%), [BF₂(CN)₂]⁻ (5%), [BF(CN)₃]⁻ (MFB, 4%), [B(CN)₄]⁻ (TCB, 6%), and an unknown borate anion (δ(¹¹B) = -20.5 ppm, 3%).

K[C₂F₅BF(CN)₂] (K2c): K2a (1.0 g, 4.4 mmol) was dissolved in Me₃SiCN (10.0 mL, 74.9 mmol). The solution was heated to 110 °C and stirred for 1 hr. During this period, the Me₃SiF that had formed was allowed to evaporate from the reaction mixture. The cylindrical reaction flask was closed and the mixture was heated to 180 °C for 30 min, cooled to room temperature, and most of the Me₃SiF that had formed was removed under reduced pressure. This procedure was repeated nine times until all the starting material was converted into the dicyanoborate according to ¹¹B and ¹⁹F NMR spectroscopy. All volatiles were distilled off and most of the excess of Me₃SiCN (7.1 mL, 53.0 mmol) was recovered and purified via distillation. The solid residue was dissolved in THF (3 mL) and addition of CH₂Cl₂ (100 mL) gave off-white K2c. The salt was filtered off and dried in a vacuum. Yield: 0.97 g (4.0 mmol, 92%). ¹³C NMR: δ = 127.8 ppm (dt, 2C, ²J(¹⁹F, ¹³C) = 35.8 Hz, ³J(¹⁹F, ¹³C) ≈ 4 Hz, CN), 121.2 ppm (qt, 1C, ¹J(¹⁹F, ¹³C) = 284.9 Hz, ²J(¹⁹F, ¹³C) = 31.9 Hz, CF₃), 117.3 ppm (tqd, 1C, ¹J(¹⁹F, ¹³C) = 258.7 Hz, ²J(¹⁹F, ¹³C) = 36.8 Hz, 30.3 Hz, CF₂). ¹¹B NMR: δ = -12.0 ppm (dt, 1B, ¹J(¹⁹F, ¹¹B) = 51.4 Hz, ²J(¹⁹F, ¹¹B) = 25.1 Hz). ¹⁹F NMR: δ = -82.6 (dt, 3F, ⁴J(¹⁹F, ¹⁹F) = 6.3 Hz, ³J(¹⁹F, ¹⁹F) = 1.0 Hz, CF₃), -132.0 (qd, 2F, ²J(¹⁹F, ¹¹B) = 25.0 Hz, ³J(¹⁹F, ¹⁹F) ≈ 5 Hz, CF₂), -219.3 ppm (qq, 1F, ¹J(¹⁹F, ¹¹B) = 51.4 Hz, ³J(¹⁹F, ¹⁹F) ≈ ⁴J(¹⁹F, ¹⁹F) = 5-6 Hz, BF). Raman: 2229, 2219 cm⁻¹ (ν(C≡N)). MALDI-MS: m/z (isotopic abundance) calcd. for 2c ([C₄BF₆N₂]⁻): 201(100), 200(25), 202(5); found: 201(100), 200(26), 202(6). Elemental analysis calcd (%) for C₄BF₆N₂: C 20.02, N 11.67; found: C 20.09, N 11.64.

K[C₂F₅BF(CN)₂] (K2c) using MW irradiation: Me₃SiCN (25.0 mL, 187.5 mmol) and K2a (8.0 g, 35.4 mmol) were stirred at room temperature for 3 days. After removal of most of the Me₃SiF, the closed reaction vessel was placed into a microwave oven (CEM Discover) and irradiated for 15 minutes (200 W, T_{max} = 78 °C). All volatiles were removed under reduced pressure and most of the excess Me₃SiCN (13.5 mL, 101.5 mmol) was recovered by fractional distillation. The solid residue was taken-up into aqueous H₂O₂ (20 mL, 30% v/v) and K₂CO₃ (5 g) was added. The solution was stirred for 1 hr, evaporated to dryness at a rotary evaporator with a bath temperature of 70 °C, and the solid remainder was extracted with ether (7×50 mL). The combined ethereal layers were dried with K₂CO₃, filtered and the solvent was removed. The solid residue was dissolved in acetone (5 mL) and colourless K2c precipitated upon addition of CH₂Cl₂ (150 mL). The solid was filtered off and dried in a vacuum. Yield: 7.8 g (32.5 mmol, 92%).

K[C₂F₅BF(CN)₂] (K2c) with Me₃SiCl: K2c was prepared according to a modified synthesis applied for K1b with Me₃SiCl using K2a (38.4 g, 170 mmol), Me₃SiCN (220 mL, 1.66 mol), and Me₃SiCl (25 mL, 198 mmol). The mixture was stirred at 80 °C for 7 hrs and K2c was isolated as an off-white sticky material. Yield: 34.3 g (143 mmol, 84%). Colourless powdery K2c was obtained from THF (50 mL) by addition of CH₂Cl₂ at -30 °C and subsequent filtration. The powder is hygroscopic and was stored under an inert atmosphere.

K[C₂F₅B(CN)₃] (K2d) using MW irradiation: K2a (0.50 g, 2.2 mmol) and Me₃SiCN (10.0 mL, 74.9 mmol) were stirred at room temperature for 2 hrs. The cylindrical reaction vessel was closed, placed into a microwave

oven (CEM Discover), and irradiated for 60 minutes (300 W, T_{\max} = 120 °C). All volatiles were removed under reduced pressure and most of the excess of Me_3SiCN (6.9 mL, 52.0 mmol) was recovered by fractional distillation. The solid residue was dissolved in aqueous H_2O_2 (10.0 mL, 30% v/v) and K_2CO_3 (2 g) was added. The mixture was stirred for 1 hr and then evaporated to dryness at a rotary evaporator at a bath temperature of 70 °C. The solid remainder was extracted with ether (4×50 mL). The combined ethereal layers were dried with K_2CO_3 , filtered, and the solvent was removed. The volume of the solution was reduced to 5 mL and colourless **K2d** precipitated upon addition of CH_2Cl_2 (150 mL). The solid was filtered off and dried in a vacuum. Yield: 0.48 g (1.9 mmol, 88%). ^{13}C NMR: δ = 123.8 (qt, 3C, $^1J(^{13}\text{C}, ^{11}\text{B})$ = 69.2 Hz, $^3J(^{19}\text{F}, ^{13}\text{C})$ = 5.3 Hz, CN), 121.3 (qt, 1C, $^1J(^{19}\text{F}, ^{13}\text{C})$ = 285.5 Hz, $^2J(^{19}\text{F}, ^{13}\text{C})$ = 32.1 Hz, CF_3), 118.4 ppm (tqt, 1C, $^1J(^{19}\text{F}, ^{13}\text{C})$ = 259.6 Hz, $^1J(^{13}\text{C}, ^{11}\text{B})$ = 63.8, $^2J(^{19}\text{F}, ^{13}\text{C})$ = 36.9 Hz, CF_2). ^{11}B NMR: δ = -32.0 ppm (t, 1B, $^2J(^{19}\text{F}, ^{11}\text{B})$ = 25.2 Hz). ^{19}F NMR: δ = -82.3 (s, 3F, CF_3), -124.2 ppm (q, 2F, $^2J(^{19}\text{F}, ^{11}\text{B})$ = 25.2 Hz, CF_2). Raman: 2236, 2232 cm^{-1} ($\nu(\text{C}\equiv\text{N})$). MALDI-MS: m/z (isotopic abundance) calcd. for **2d** ($[\text{C}_5\text{BF}_5\text{N}_3]^+$): 208(100), 207(24), 209(7); found: 208(100), 207(25), 209(5). Elemental analysis calcd (%) for $\text{C}_5\text{BF}_5\text{KN}_3$: C 24.32, N 17.01; found: C 24.53, N 16.79.

K[C₂F₅B(CN)₃] (K2d) with Et₃SiCN: K2a (2.60 g, 11.5 mmol) was dissolved in Et_3SiCN (25.0 mL, 140 mmol). Et_3SiCl (2 mL, 11.9 mmol) was added and the reaction mixture was degassed. The vessel was closed and heated to 190 °C for 16 hrs. All volatiles were removed under reduced pressure and most of the excess of Et_3SiCN (15 mL, 86.7 mmol) was recovered by fractional distillation. The solid residue was taken-up into aqueous H_2O_2 (15 mL, 30% v/v) and K_2CO_3 (3 g) was added. The solution was stirred for several hours, evaporated to dryness at a rotary evaporator, and the solid remainder was extracted with acetone (4×50 mL). The volume of the combined organic layers was concentrated to 5 mL and addition of CH_2Cl_2 (100 mL) gave off-white **K2d**. The salt was filtered off and dried in a vacuum. Yield: 2.1 g (8.5 mmol, 74%).

K[C₂F₅B(CN)₃] (K2d) with Me₃SiCl using an autoclave: The procedure applied for the preparation of **K2d** was similar to the one described for the synthesis of **K1d** (Me_3SiCl /autoclave). **K2a** (41.0 g, 182 mmol), Me_3SiCN (220 mL, 1.65 mol), and Me_3SiCl (15.0 mL, 119 mmol) were used as starting materials. The maximum pressure during the reaction was approximately 20 bar. Off-white **K2d** was obtained by addition of CHCl_3 (200 mL) to a solution in acetone (10 mL). Yield: 38.3 g (155 mmol, 85%).

K[C₂F₅B(CN)₃] (K2d) starting from Na2a in an autoclave: The procedure used for the preparation of **K2d** was similar to the one described for the synthesis of **K1d** with Me_3SiCl in an autoclave starting from **Na2a** (25.0 g, 119 mmol), Me_3SiCN (210 mL, 1.58 mol), and Me_3SiCl (15.0 mL, 119 mmol). After 9 hrs the reaction was completed and the maximum pressure was approximately 15 bar. Yield: 27.0 g (109 mmol, 92%).

K[C₃F₇BF₂(CN)] (K3b): The procedure used for the preparation of **K3b** was similar to the one described for the synthesis of **K1b** with Me_3SiCl . **K3a** (2.72 g, 9.86 mmol), Me_3SiCN (20.0 mL, 150 mmol), and Me_3SiCl (1.0 mL, 7.86 mmol) were used as starting compounds. Yield: 2.60 g (9.19 mmol, 93%). ^{13}C NMR: δ = 130.5 (qt, 1C, $^1J(^{13}\text{C}, ^{11}\text{B})$ = 76.8 Hz, $^2J(^{19}\text{F}, ^{13}\text{C})$ = 49.0 Hz, CN), 120.0 (tqt, 1C, $^1J(^{19}\text{F}, ^{13}\text{C})$ = 261.2 Hz, $^1J(^{13}\text{C}, ^{11}\text{B})$ = 77.3 Hz, $^2J(^{19}\text{F}, ^{13}\text{C})$ = 41.6 Hz, 34.1 Hz, BCF_2), 119.5 (qt, 1C, $^1J(^{19}\text{F}, ^{13}\text{C})$ = 287.1 Hz, $^2J(^{13}\text{C}, ^{19}\text{F})$ = 35.3 Hz, CF_3), 111.9 ppm (tqt, 1C, $^1J(^{19}\text{F}, ^{13}\text{C})$ = 259.5 Hz, $^2J(^{19}\text{F}, ^{13}\text{C})$ = 36.3 Hz, 31.3 Hz, CF_2). ^{11}B NMR: δ = -2.6 ppm (tt, 1B, $^1J(^{19}\text{F}, ^{11}\text{B})$ = 51.1 Hz, $^2J(^{19}\text{F}, ^{11}\text{B})$ = 23.4 Hz). ^{19}F NMR: δ = -81.7 (tt, 3F, $^3J(^{19}\text{F}, ^{19}\text{F})$ = 9.5 Hz, $^4J(^{19}\text{F}, ^{19}\text{F})$ = 2.9 Hz, CF_3), -127.9 (tm, 2F, $^3J(^{19}\text{F}, ^{19}\text{F})$ = 6 Hz, CF_2), -133.8 (m, 2F, BCF_2), -166.3 ppm (q, 2F, $^1J(^{19}\text{F}, ^{11}\text{B})$ = 51.0 Hz, BF_2). Raman: 2235, 2226, 2219 cm^{-1} ($\nu(\text{C}\equiv\text{N})$). Elemental analysis calcd (%) for $\text{C}_4\text{BF}_9\text{KN}$: C 16.98, N 4.95; found: C 18.62, N 5.17.

K[C₄F₉BF₂(CN)] (K4b): **K4b** was synthesized similar to **K1b** with Me_3SiCl starting from **K4a** (2.85 g, 8.74 mmol), Me_3SiCN (20.0 mL, 150 mmol) and Me_3SiCl (1.0 mL, 7.86 mmol). Yield: 2.57 g (7.7 mmol, 88%). ^{13}C NMR: δ = 130.6 (qt, 1C, $^1J(^{13}\text{C}, ^{11}\text{B})$ = 76.7 Hz, $^2J(^{19}\text{F}, ^{13}\text{C})$ = 49.1 Hz, CN), 120.7 (qm, 1C, $^1J(^{13}\text{C}, ^{11}\text{B})$ = 77.1 Hz, BCF_2), 118.8 (qt, 1C, $^1J(^{19}\text{F}, ^{13}\text{C})$ = 287.2 Hz, $^2J(^{19}\text{F}, ^{13}\text{C})$ = 33.9 Hz, CF_3), 113.6 (tm, 1C, $^1J(^{19}\text{F}, ^{13}\text{C})$ =

260.4 Hz, BCF_2CF_2), 110.2 ppm (tqt, 1C, $^1J(^{19}\text{F}, ^{13}\text{C})$ = 267.0 Hz, $^2J(^{19}\text{F}, ^{13}\text{C})$ = 37.9 Hz, 34.8 Hz, CF_2CF_3). ^{11}B NMR: δ = -2.6 (tt, 1B, $^1J(^{19}\text{F}, ^{11}\text{B})$ = 51.1 Hz, $^2J(^{19}\text{F}, ^{11}\text{B})$ = 23.3 Hz). ^{19}F NMR: δ = -82.0 (tt, 3F, $^3J(^{19}\text{F}, ^{19}\text{F})$ = 9.8 Hz, $^4J(^{19}\text{F}, ^{19}\text{F})$ = 3.8 Hz, CF_3), -124.2 (m, 2F, CF_2), -127.0 (tm, 2F, $^3J(^{19}\text{F}, ^{19}\text{F})$ = 12.7 Hz, CF_2), -133.2 (m, 2F, BCF_2), -166.0 (q, 2F, $^1J(^{19}\text{F}, ^{11}\text{B})$ = 51.0 Hz, BF_2). Raman: 2236 cm^{-1} ($\nu(\text{C}\equiv\text{N})$). Elemental analysis calcd (%) for $\text{C}_5\text{BF}_{11}\text{KN}$: C 18.04, N 4.21; found: C 18.86, N 4.68.

K[C₄F₉BF(CN)₂] (K4c): The procedure used for the preparation of **K4c** was similar to the one described for the synthesis of **K2c**. The yield was not determined. ^{13}C NMR: δ = 128.1 (qd, 2C, $^1J(^{13}\text{C}, ^{11}\text{B})$ = 72 Hz, $^2J(^{19}\text{F}, ^{13}\text{C})$ = 35.7 Hz, CN), 120.6 (tqt, 1C, $^1J(^{19}\text{F}, ^{11}\text{B})$ = 261 Hz, $^1J(^{13}\text{C}, ^{11}\text{B})$ = 72 Hz, $^2J(^{19}\text{F}, ^{11}\text{B})$ = 36.0 Hz, 30.7 Hz, BCF_2), 118.5 (qt, 1C, $^1J(^{19}\text{F}, ^{13}\text{C})$ = 287.2 Hz, $^2J(^{19}\text{F}, ^{13}\text{C})$ = 33.7 Hz, CF_3), 113.3 (tm, 1C, $^1J(^{19}\text{F}, ^{13}\text{C})$ = 261.1 Hz, BCF_2CF_2), 110.0 ppm (tqt, 1C, $^1J(^{19}\text{F}, ^{13}\text{C})$ = 267.4 Hz, $^2J(^{19}\text{F}, ^{13}\text{C})$ = 38.3 Hz, 34.4 Hz, CF_2CF_3). ^{11}B NMR: δ = -11.8 ppm (dt, 1B, $^1J(^{19}\text{F}, ^{11}\text{B})$ = 51.5 Hz, $^2J(^{19}\text{F}, ^{11}\text{B})$ = 25.1 Hz). ^{19}F NMR: δ = -82.1 (tt, 3F, $^3J(^{19}\text{F}, ^{19}\text{F})$ = 9.8 Hz, $^4J(^{19}\text{F}, ^{19}\text{F})$ = 3.8 Hz, CF_3), -122.6 (m, 2F, CF_2), -127.0 (tm, 2F, $^3J(^{19}\text{F}, ^{19}\text{F})$ = 13.5 Hz, CF_2), -128.7 (m, 2F, BCF_2), -218.0 (q, 1F, $^1J(^{19}\text{F}, ^{11}\text{B})$ = 51.3 Hz, BF).

Salt Metathesis

Standard protocol: The potassium borate was dissolved in deionized water (10–50 mL) and an aqueous solution that contains a slight excess of $[\text{Kat}]\text{Hal}$ (1.1–1.2 equivalents; $[\text{Kat}]^+ = [\text{EMIm}]^+$, $[\text{nBu}_4\text{N}]^+$, $[\text{Ph}_4\text{P}]^+$, ...; $\text{Hal}^- = \text{Cl}^-$, Br^- , I^-) was added, slowly. The IL was either separated as a liquid that usually separated at the bottom of the flask or it was obtained via extraction using CH_2Cl_2 (3× 20–50 mL). The IL or a solution thereof in an organic solvent was washed with deionized water (5× 1–5 mL). All volatiles were removed under reduced pressure to yield the IL that was dried in a vacuum at 40–60 °C overnight. Solid salts were separated by filtration, washed with water and dried in a vacuum.

Experimental details including spectroscopic data for cyanoborates with organic cations are given in the Supporting Information.

Diffusion-ordered Spectroscopy (DOSY): ^1H , ^{19}F , ^{11}B , and ^{13}C DOSY measurements were performed at 20, 40, and 60 °C (^{13}C only at 20 °C) in 5 mm NMR tubes on a Bruker Avance III HD 600 spectrometer equipped with a 5 mm BBFO probe ($^1\text{H}/\text{X}$ with $\text{X} = ^{15}\text{N}$, ^{31}P and ^{19}F) with z axis gradient coil capable of producing pulsed magnetic field gradients of 50 G/cm. The pure ILs were investigated, locking and shimming were executed by use of a coaxial inlet filled with DMSO-d₆ and centred in the NMR tube. Temperature calibration was performed with standard samples of 0.2% CH_3OH in CD_3OD and 80% ethylene glycole in DMSO-d₆. Data were acquired and processed using the Bruker software Topspin 3.2. The DOSY data were recorded with the stimulated echo BPP-LED pulse sequence^[76] (longitudinal eddy current delay sequence with bipolar gradient pulse pairs for diffusion and additional spoil gradients after the second and fourth 90° pulse). The diffusion time Δ was kept constant in each DOSY experiment while the smoothed square diffusion gradients were incremented from 2 to 98% of maximum gradient strength in 32 linear steps (except for ^{13}C DOSY, due to limited signal/noise ratio only 16 steps were used). No decoupling was used to avoid heating of the sample. In samples with more than one ^{19}F signal, ^{19}F DOSY measurements were performed for each signal individually to avoid experimental errors due to non-uniform excitation in the large ^{19}F chemical shift range. One component fittings of the gradient strength dependence of the signal intensities were performed by a Levenberg-Marquardt algorithm incorporated in the Bruker software Topspin 3.2. The experimental intensities show no systematic and only very small random deviations from a Gaussian decay curve. Since the viscosity of the ILs is high as compared with organic solvents and no cryoprobe was used it was not expected that the DOSY results were influenced by convection effects. To verify this, for all of the samples (except for $[\text{EMIm}]\text{TBCB}$) the DOSY measurements at 60 °C were performed with different diffusion times Δ or by use of the corresponding double stimulated echo pulse sequence^[77] (with spoil gradients after the second, fourth, and sixth 90° pulse) in which the double stimulated echo results in a compensation of possible flow effects. No dependence of the

experimentally determined diffusion coefficient on the diffusion time Δ and identical results for the stimulated and the double stimulated echo sequence were observed.

Electrochemical Measurements: All electrochemical studies were performed on the neat ILs under an Argon atmosphere with a Metrohm PGSTAT30 potentiostat and a Microcell HC set-up with a Eurotherm temperature controller (rhd instruments). A 0.1 mL Pt-cell TSC-70 closed (rhd instruments) served as counter electrode and was equipped with a glassy carbon working electrode (surface area: $3.14 \cdot 10^{-2} \text{ cm}^2$). Specific conductivities (σ) were determined at different temperatures (20, 40, 60, 70, 80 °C) by impedance spectroscopy from $500 \cdot 10^3$ to 800 Hz. The cell constant was determined on a $1413 \mu\text{S}\cdot\text{cm}^{-1}$ conductivity solution HI 70031 (HANNA instruments). Cyclic voltammetry was conducted at 20 °C with a scan rate of $50 \text{ mV}\cdot\text{s}^{-1}$ using the same set-up and an additional Ag/Ag⁺ micro reference electrode (acetonitrile, rhd instruments).

Single-Crystal X-ray Diffraction: Colourless single crystals of **K1b**, **K1c**, **K1d**, **K2d**-Me₂CO, **[nBu₄N]2c**, **K3b**-0.33Me₂CO, and **K4c**-Me₂CO suitable for X-ray diffraction were obtained from acetone solutions by slow evaporation of the solvent. Crystals of **K1b**, **K1c**, **K1d**, and **[nBu₄N]2c** were investigated with an imaging plate diffraction system (IPDS, Stoe & Cie), a crystal of **K2d**-Me₂CO was studied with an Oxford Xcalibur diffractometer equipped with an EOS detector, and crystals of **K3b**-0.33Me₂CO and **K4c**-Me₂CO were studied on a Bruker X8-Apex II diffractometer with a CCD area detector and multi-layer mirror or graphite monochromated using Mo-K α radiation ($\lambda = 0.71073 \text{ \AA}$). All structures were solved by direct methods,^[78,79] and refinements are based on full-matrix least-squares calculations on F^2 .^[78,80] All non-hydrogen atoms were refined anisotropically. The positions of all H atoms were located from electron density difference maps. In the final steps of the refinements, idealized bond lengths and angles were introduced, and the isotropic displacement parameters were kept equal to 150% for H atoms of methyl groups and to 120% for H atoms of CH₂ groups.

All calculations were performed with the WinGX program package^[81] or using the ShelXle graphical interface.^[82] Molecular structure diagrams were drawn with the program Diamond 4.3.2.^[83] Selected bond parameters are summarized in Tables S7 and S8 in the Supporting Information. Experimental details, crystal data, and the CCDC numbers are collected in Table S6 in the Supporting Information. These data can be obtained free of charge from The Cambridge Crystallographic Data Centre via www.ccdc.cam.ac.uk/data_request/cif.

DFT Calculations: Density functional calculations (DFT)^[84] using the hybrid functional B3LYP^[85] and Pople-type basis sets 6-311+G(d) were performed with the Gaussian09 program suite.^[86] All structures represent true minima with no imaginary frequency on the respective hypersurface.

Acknowledgements

Financial support by Merck KGaA (Darmstadt, Germany) and the Deutsche Forschungsgemeinschaft (DFG, SPP 1708, FI 1628/4-2) is gratefully acknowledged. The authors thank Prof. G. Sextl, Mrs. C. Wendler and Mr. R. Olsowski (all Fraunhofer-Institut für Silicatforschung (ISC), Würzburg, Germany) Mrs. A. Amann (Merck KGaA, Darmstadt, Germany), Dr. K. Kawata, Dr. H. Yoshizaki and Dr. H. Shinohara (Merck Ltd. Japan), Prof. W. Frank, Mrs. E. Hammes, Mr. P. Roloff and Dr. P. Tommes (all Universität Düsseldorf, Germany) as well as Mrs. Patricia Altenberger and Mrs. Juliane Adelmann (all Universität Würzburg, Germany) for technical support.

Keywords: borates • perfluoroalkylborates • ionic liquids • viscosity • conductivity

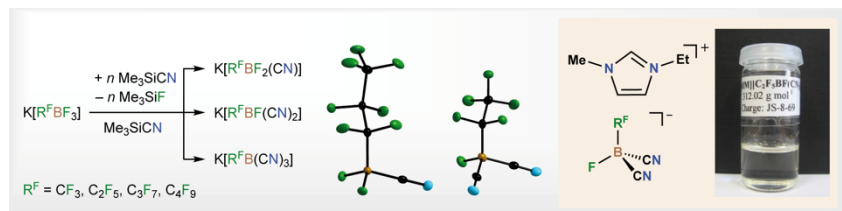
- [1] N. V. Ignat'ev, M. Finze, J. A. P. Sprenger, C. Kerpen, E. Bernhardt, H. Willner, *J. Fluorine Chem.* **2015**, *177*, 46–54.
- [2] *Ionic Liquids in Synthesis*, 2nd ed., P. Wasserscheid, T. Welton, Wiley-VCH Verlag GmbH & Co. KGaA, Weinheim, **2007**; *Ionic Liquids UnCOILed: Critical Expert Overviews: COILed for Action*, John Wiley & Sons, Inc., Hoboken, New Jersey, **2013**; *Electrochemical Aspects of Ionic Liquids*, 2nd ed., John Wiley & Sons, Inc., Hoboken, New Jersey, **2011**; *Electrodeposition from Ionic Liquids*, Wiley-VCH Verlag GmbH & Co. KGaA, Weinheim, **2008**; M. Watanabe, M. L. Thomas, S. Zhang, K. Ueno, T. Yasuda, K. Dokko, *Chem. Rev.* **2017**, *117*, 7190–7239; S. Zhang, Q. Zhang, Y. Zhang, Z.-N. Chen, M. Watanabe, Y. Deng, *Prog. Mater. Sci.* **2016**, *77*, 80–124; T. Welton, *Proc. R. Soc. London, A* **2015**, *471*, 20150502; J. P. Hallett, T. Welton, *Chem. Rev.* **2011**, *111*, 3508–3576; M. Armand, F. Endres, D. R. MacFarlane, H. Ohno, B. Scrosati, *Nat. Mater.* **2009**, *8*, 621–629; K. S. Egorova, E. G. Gordeev, V. P. Ananikov, *Chem. Rev.* **2017**, *117*, 7132–7189; P. Wasserscheid, W. Keim, *Angew. Chem.* **2000**, *112*, 3926–3945; *Angew. Chem. Int. Ed.* **2000**, *39*, 3772–3789; M. Deetlefs, M. Fanselow, K. R. Seddon, *RSC Adv.* **2016**, *6*, 4280–4288; N. V. Plechkova, K. R. Seddon, *Chem. Soc. Rev.* **2008**, *37*, 123–150; R. D. Rogers, K. R. Seddon, *Science* **2003**, *792*, 792–793.
- [3] E. Bernhardt, G. Henkel, H. Willner, *Z. Anorg. Allg. Chem.* **2000**, *626*, 560–568.
- [4] D. J. Williams, B. Pleune, J. Kouvetakis, M. D. Williams, R. A. Andersen, *J. Am. Chem. Soc.* **2000**, *122*, 7735–7741.
- [5] E. Bernhardt, M. Finze, H. Willner, *Z. Anorg. Allg. Chem.* **2003**, *629*, 1229–1234.
- [6] U. Welz-Biermann, N. Ignatyev, E. Bernhardt, M. Finze, H. Willner, Merck Patent GmbH, WO2004072089, 2004.
- [7] R. Koerver, D. MacFarlane, J. M. Pringle, *Electrochim. Acta* **2015**, *184*, 186–192; J. X. Mao, A. S. Lee, J. R. Kitchin, H. B. Nulwala, L. D. R., K. Damodaran, *J. Mol. Struct.* **2013**, *1038*, 12–18; H. F. D. Almeida, P. J. Carvalho, K. A. Kurnia, J. A. Lopes-da-Silva, J. A. P. Coutinho, M. G. Freire, *Fluid Phase Equilib.* **2016**, *409*, 458–465; T. M. Koller, M. H. Rausch, K. Pohako-Esko, P. Wasserscheid, A. P. Fröba, *J. Chem. Eng. Data* **2015**, *60*, 2665–2673; T. M. Koller, M. H. Rausch, P. S. Schulz, M. Berger, P. Wasserscheid, I. G. Economou, A. Leipertz, A. P. Fröba, *J. Chem. Eng. Data* **2012**, *57*, 828–835; K. R. Harris, M. Kanakubo, *J. Chem. Eng. Data* **2016**, *61*, 2399–2411; H. Weber, B. Kirchner, *J. Phys. Chem. B* **2016**, *120*, 2471–2483; T. M. Koller, J. Ramos, P. S. Schulz, I. G. Economou, M. H. Rausch, A. P. Fröba, *J. Phys. Chem. B* **2017**, *121*, 4145–4157; J. Tong, Q.-S. Liu, Y.-X. Fang, D.-W. Fang, U. Welz-Biermann, J.-Z. Yang, *J. Chem. Eng. Data* **2010**, *55*, 3693–3696; T. M. Koller, M. D. Rausch, J. Ramos, P. S. Schulz, P. Wasserscheid, I. G. Economou, A. P. Fröba, *J. Phys. Chem. B* **2013**, *117*, 8512–8523; C. M. S. S. Neves, K. A. Kurnia, J. A. P. Coutinho, I. M. Marrucho, J. N. Canongia Lopes, M. G. Freire, L. P. N. Rebelo, *J. Phys. Chem. B* **2013**, *117*, 10271–10283.
- [8] D. Kuang, P. Wang, S. M. Zakeeruddin, M. Grätzel, Ecole Polytechnique Federale de Lausanne (EPFL), WO2007093961, 2007; D. Kuang, P. Wang, S. Ito, S. M. Zakeeruddin, M. Grätzel, *J. Am. Chem. Soc.* **2006**, *128*, 7732–7733.
- [9] M. Marszalek, Z. Fei, D.-R. Zhu, R. Scopelliti, P. J. Dyson, S. M. Zakeeruddin, M. Grätzel, *Inorg. Chem.* **2011**, *50*, 11561–11567.
- [10] N. Ignatyev, M. Schulte, K. Kawata, T. Goto, E. Bernhardt, V. Bernhardt-Pitchougina, H. Willner, Merck Patent GmbH, WO2012163489, 2012; N. Ignatyev, M. Schulte, E. Bernhardt, V. Bernhardt-Pitchougina, H. Willner, Merck Patent GmbH, WO2012163488, 2012; K. Kawata, T. Goto, N. Ignatyev, M. Schulte, H. Yoshizaki, E. Bernhardt, V. Bernhardt-Pitchougina, H. Willner, Merck Patent GmbH, WO2012163490, 2012; Y. Zhang, J. M. Shreeve, *Angew. Chem.* **2011**, *123*, 965–967; *Angew. Chem. Int. Ed.* **2011**, *50*, 935–937; Q. Zhang, J. M. Shreeve, *Chem. Rev.* **2014**, *114*, 10527–10574.
- [11] M. Nazeeruddin, M. Grätzel, E. Baranoff, F. Kessler, J.-H. Yum, A. Yella, H. N. Tsao, Ecole Polytechnique Federale de Lausanne (EPFL), WO2012114315A1, 2012; H. N. Tsao, P. Comte, C. Yi, M. Grätzel, *ChemPhysChem* **2012**, *13*, 2976–2981.
- [12] F. Falk, L. Hackbarth, S. Lochbrunner, H. Marciniak, M. Köckerling, *Eur. J. Inorg. Chem.* **2016**, 469–476.

- [13] M. Finze, E. Bernhardt, M. Berkei, H. Willner, J. Hung, R. M. Waymouth, *Organometallics* **2005**, *24*, 5103–5109.
- [14] T. Küppers, E. Bernhardt, C. W. Lehmann, H. Willner, *Z. Anorg. Allg. Chem.* **2007**, *633*, 1666–1672.
- [15] A. Kütt, T. Rodima, J. Saame, E. Raamat, V. Mäemets, I. Kaljurand, I. A. Koppel, R. Y. Gariyuskayte, Y. L. Yagupolskii, L. M. Yagupolskii, E. Bernhardt, H. Willner, I. Leito, *J. Org. Chem.* **2011**, *76*, 391–395.
- [16] E. Bernhardt, M. Finze, H. Willner, *Inorg. Chem.* **2011**, *50*, 10268–10273.
- [17] E. Bernhardt, G. Henkel, H. Willner, G. Pawelke, H. Bürger, *Chem. Eur. J.* **2001**, *7*, 4696–4705.
- [18] E. Bernhardt, D. J. Brauer, M. Finze, H. Willner, *Angew. Chem.* **2006**, *118*, 6532–6534; *Angew. Chem., Int. Ed. Engl.* **2006**, *45*, 6383–6386.
- [19] E. Bernhardt, V. Bernhardt-Pitchougina, H. Willner, N. V. Ignatiev, *Angew. Chem.* **2011**, *123*, 12291–12294; *Angew. Chem. Int. Ed.* **2011**, *50*, 12085–12088.
- [20] J. Landmann, J. A. P. Sprenger, R. Bertermann, N. Ignat'ev, V. Bernhardt-Pitchougina, E. Bernhardt, H. Willner, M. Finze, *Chem. Commun.* **2015**, *51*, 4989–4992.
- [21] J. Landmann, F. Keppner, D. B. Hofmann, J. A. P. Sprenger, M. Häring, S. H. Zöttnick, K. Müller-Buschbaum, N. V. Ignat'ev, M. Finze, *Angew. Chem.* **2017**, *129*, 2839–2843; *Angew. Chem. Int. Ed.* **2017**, *56*, 2795–2799; J. Landmann, F. Keppner, J. A. P. Sprenger, M. Finze, N. Ignat'ev, Julius-Maximilians-Universität Würzburg, Merck Patent GmbH, DE102014018103A1, 2016.
- [22] J. Landmann, J. A. P. Sprenger, M. Hailmann, V. Bernhardt-Pitchougina, H. Willner, N. Ignat'ev, E. Bernhardt, M. Finze, *Angew. Chem.* **2015**, *127*, 11411–11416; *Angew. Chem. Int. Ed.* **2015**, *54*, 11259–11264; J. A. P. Sprenger, J. Landmann, M. Finze, V. Bernhardt-Pitchougina, N. Ignatiev, E. Bernhardt, H. Willner, Merck Patent GmbH, WO2015022048, 2015.
- [23] N. Y. Adonin, V. V. Bardin, *Russ. Chem. Rev.* **2010**, *79*, 757–785.
- [24] M. Finze, E. Bernhardt, H. Willner, *Angew. Chem.* **2007**, *119*, 9340–9357; *Angew. Chem. Int. Ed.* **2007**, *46*, 9180–9196.
- [25] G. Pawelke, H. Bürger, *Coord. Chem. Rev.* **2001**, *215*, 243–266; G. Pawelke, H. Bürger, *Appl. Organomet. Chem.* **1996**, *10*, 147–174.
- [26] E. Bernhardt, M. Berkei, H. Willner, *Z. Anorg. Allg. Chem.* **2009**, *635*, 2009–2015.
- [27] I. Krossing, I. Raabe, *Angew. Chem.* **2004**, *116*, 2116–2142; *Angew. Chem., Int. Ed. Engl.* **2004**, *43*, 2066–2090.
- [28] T. A. Engesser, C. Friedmann, A. Martens, D. Kratzert, P. J. Malinowski, I. Krossing, *Chem. Eur. J.* **2016**, *22*, 15085–15094.
- [29] E. Bernhardt, M. Finze, H. Willner, C. W. Lehmann, F. Aubke, *Chem. Eur. J.* **2006**, *12*, 8276–8283.
- [30] W. W. Wilson, A. Vij, V. Vij, E. Bernhardt, K. O. Christe, *Chem. Eur. J.* **2003**, *9*, 2840–2844.
- [31] E. Bernhardt, M. Finze, H. Willner, *Z. Anorg. Allg. Chem.* **2006**, *632*, 248–250.
- [32] M. Schmidt, A. Kühner, H. Willner, E. Bernhardt, Merck Patent GmbH, EP1205480(A2), 2002.
- [33] N. Y. Adonin, V. V. Bardin, H.-J. Frohn, *Z. Anorg. Allg. Chem.* **2007**, *633*, 647–652.
- [34] S. Darses, J.-P. Genet, *Eur. J. Org. Chem.* **2003**, 4313–4327.
- [35] Z.-B. Zhou, H. Matsumoto, K. Tatsumi, *Chem. Eur. J.* **2004**, *10*, 6581–6591.
- [36] Z. B. Zhou, H. Matsumoto, K. Tatsumi, *Chem. Eur. J.* **2005**, *11*, 752–766; Z.-B. Zhou, H. Matsumoto, K. Tatsumi, *ChemPhysChem* **2005**, *6*, 1324–1332; Z.-B. Zhou, M. Takeda, M. Ue, *J. Fluorine Chem.* **2004**, *125*, 461–476; Z.-B. Zhou, H. Matsumoto, K. Tatsumi, *Chem. Eur. J.* **2006**, *12*, 2196–2212; Z.-B. Zhou, H. Matsumoto, K. Tatsumi, *Chem. Lett.* **2004**, *33*, 886–887; Z.-B. Zhou, H. Matsumoto, K. Tatsumi, *Chem. Lett.* **2004**, *33*, 1636–1637.
- [37] N. V. Ignatiev, U. Welz-Biermann, G. Bissky, H. Willner, A. Kucheryna, Merck Patent GmbH, WO2005105815, 2005.
- [38] Z.-B. Zhou, M. Takeda, T. Fujii, M. Ue, *J. Electrochem. Soc.* **2005**, *152*, A351–A356; M. Ue, T. Fujii, Z.-B. Zhou, M. Takeda, S. Kinoshita, *Solid State Ionics* **2006**, *177*, 323–331.
- [39] Z.-B. Zhou, M. Takeda, M. Ue, *J. Fluorine Chem.* **2003**, *123*, 127–131.
- [40] T. Knauber, F. Arian, G.-V. Rösenthaler, L. J. Gooßen, *Chem. Eur. J.* **2011**, *17*, 2689–2697; B. A. Khan, A. E. Buba, L. J. Gooßen, *Chem. Eur. J.* **2012**, *18*, 1577–1581; Z. Gonda, A. Kovács, C. Wéber, T. Gáti, A. Mészáros, A. Kotschy, Z. Novák, *Org. Lett.* **2014**, *16*, 4268–4271; T. Sugiyoshi, D. Kawachi, M. Sato, T. Sakai, H. Amii, *Synthesis* **2017**, *49*, 1874–1878; V. V. Levin, A. D. Dilman, P. A. Belyakov, M. I. Struchkova, V. A. Tartakovsky, *Tetrahedron Lett.* **2011**, *52*, 281–284.
- [41] H.-J. Frohn, V. V. Bardin, *Z. Anorg. Allg. Chem.* **2001**, *627*, 15–16.
- [42] G. A. Molander, B. P. Hoag, *Organometallics* **2003**, *22*, 3313–3315.
- [43] J. A. P. Sprenger, M. Finze, N. Ignatiev, Merck Patent GmbH, WO2016074756, 2016.
- [44] M. Finze, E. Bernhardt, H. Willner, C. W. Lehmann, *J. Am. Chem. Soc.* **2005**, *127*, 10712–10722.
- [45] M. Finze, E. Bernhardt, H. Willner, C. W. Lehmann, *Inorg. Chem.* **2006**, *45*, 669–678.
- [46] M. Finze, E. Bernhardt, H. Willner, C. W. Lehmann, *Organometallics* **2006**, *25*, 3070–3075.
- [47] M. Finze, E. Bernhardt, H. Willner, N. V. Ignatiev, U. Welz-Biermann, Merck Patent GmbH, WO2006045405, 2006.
- [48] T. Ribbeck, S. H. Zöttnick, C. Kerpen, J. Landmann, N. V. Ignat'ev, K. Müller-Buschbaum, M. Finze, *Inorg. Chem.* **2017**, *56*, 2278–2286.
- [49] N. Ignatiev, M. Schulte, J. Sprenger, M. Finze, W. Frank, Merck Patent GmbH, WO2011085966, 2011.
- [50] K. Kawata, H. Yoshizaki, H. Shinohara, P. Kirsch, N. Ignatiev, M. Schulte, J. Sprenger, M. Finze, W. Frank, Merck Patent GmbH, WO2011085965, 2011.
- [51] J. A. P. Sprenger, J. Landmann, M. Drisch, N. Ignat'ev, M. Finze, *Inorg. Chem.* **2015**, *54*, 3403–3412.
- [52] M. G. Voronkov, V. K. Roman, E. A. Maletina, *Synthesis* **1982**, 277–280.
- [53] K. Mai, G. Patil, *J. Org. Chem.* **1986**, *51*, 3545–3548.
- [54] M. R. Detty, M. D. Seidler, *J. Org. Chem.* **1981**, *46*, 1283–1292.
- [55] J. A. Gierut, F. J. Sow, J. A. Nieuwland, *J. Am. Chem. Soc.* **1936**, *58*, 897–898.
- [56] D. J. Brauer, H. Bürger, G. Pawelke, *Inorg. Chem.* **1977**, *16*, 2305–2314.
- [57] S. Higashiya, A. S. Filatov, C. C. Wells, M. V. Rane-Fondacaro, P. Haldar, *J. Mol. Struct.* **2010**, *984*, 300–306.
- [58] M. Finze, E. Bernhardt, M. Záhres, H. Willner, *Inorg. Chem.* **2004**, *43*, 490–505.
- [59] M. Finze, E. Bernhardt, A. Terheiden, M. Berkei, H. Willner, D. Christen, H. Oberhammer, F. Aubke, *J. Am. Chem. Soc.* **2002**, *124*, 15385–15398; P. S. Hubbard, *J. Chem. Phys.* **1970**, *53*, 985–987; T. K. Halstead, P. A. Osment, B. C. Sanctuary, J. Tangenfeldt, I. J. Lowe, *J. Magn. Reson.* **1986**, *67*, 267–306; A. Abragam, *Principles of Nuclear Magnetism*, Clarendon Press, Oxford, U. K., **1986**; P. Bendel, *J. Magn. Reson.* **1995**, *A 117*, 143–149.
- [60] V. Daněk, I. Votava, M. Chrenková-Paučířová, K. Matiašovský, *Chem. Zvesti* **1976**, *30*, 841–846.
- [61] P. Barthen, W. Frank, N. Ignatiev, *Ionics* **2015**, *21*, 149–159.
- [62] M. Galiński, A. Lewandowski, I. Stępnik, *Electrochim. Acta* **2006**, *51*, 5567–5580.
- [63] P. Bonhôte, A.-P. Dias, N. Papageorgiou, K. Kalyanasundaram, M. Grätzel, *Inorg. Chem.* **1996**, *35*, 1168–1178.
- [64] C. A. Angell, Y. Ansari, Z. Zhao, *Faraday Discuss.* **2012**, *154*, 9–27; W. Xu, E. I. Cooper, C. A. Angell, *J. Phys. Chem. B* **2003**, *107*, 6170–6178; C. A. Angell, N. Byrne, J.-P. Belieres, *Acc. Chem. Res.* **2007**, *40*, 1228–1236.
- [65] A. Noda, M. A. B. H. Susan, K. Kudo, S. Mitsushima, K. Hayamizu, M. Watanabe, *J. Phys. Chem. B* **2003**, *107*, 4024–4033; K. Ueno, H. Tokuda, M. Watanabe, *Phys. Chem. Chem. Phys.* **2010**, *12*, 1649–1658; O. Hollóczki, F. Malberg, T. Welton, B. Kirchner, *Phys. Chem. Chem. Phys.* **2014**, *16*, 16680–16890; D. R. MacFarlane, M. Forsyth, E. I. Izgorodina, A. P. Abbott, G. Annat, K. Fraser, *Phys. Chem. Chem. Phys.* **2009**, *11*, 4962–4967.
- [66] H. Vogel, *Phys. Z.* **1921**, *22*, 645–646; G. S. Fulcher, *J. Am. Ceram. Soc.* **1925**, *8*, 339–355; G. Tammann, W. Hesse, *Z. Anorg. Allg. Chem.* **1926**, *156*, 245–257.
- [67] J. O. M. Bockris, A. K. Reddy, *Modern Electrochemistry, Vol. 1*, **1970**.
- [68] T. A. Litovitz, *J. Chem. Phys.* **1952**, *20*, 1088–1089.
- [69] B. O'Regan, M. Grätzel, *Nature (London)* **1991**, *353*, 737–740.
- [70] R. K. Harris, E. D. Becker, S. M. Cabral de Menezes, R. Goodfellow, P. Granger, *Pure Appl. Chem.* **2001**, *73*, 1795–1818.

- [71] G. R. Fulmer, A. J. M. Miller, N. H. Sherden, H. E. Gottlieb, A. Nudelman, B. M. Stoltz, J. E. Bercaw, K. I. Goldberg, *Organometallics* **2010**, *29*, 2176–2179.
- [72] W. L. F. Armarego, C. L. L. Chai, *Purification of Laboratory Chemicals*, 5 ed., Butterworth-Heinemann (Elsevier), **2003**.
- [73] N. V. Ignatiev, U. Welz-Biermann, G. Bissky, H. Willner, A. Kucheryna, Merck Patent GmbH, WO2005105815, 2005.
- [74] A. A. Kolomeitsev, A. A. Kadyrov, J. Szczepkoska-Sztolcman, M. Milewska, H. Koroniak, G. Bissky, J. A. Barten, G.-V. Rösenthaller, *Tetrahedron Lett.* **2003**, *44*, 8273–8277.
- [75] M. Arend, *J. Prakt. Chem.* **1998**, *340*, 760–763.
- [76] D. Wu, A. Chen, C. S. Johnson Jr., *J. Magn. Reson. A* **1995**, *115*, 260–264.
- [77] A. Jerschow, N. Müller, *J. Magn. Reson.* **1997**, *125*, 375–375.
- [78] G. M. Sheldrick, *Acta Crystallogr.* **2008**, *A64*, 112–122.
- [79] SHELXS-97, Program for Crystal Structure Solution, G. M. Sheldrick, Universität Göttingen, 1997.
- [80] SHELXL-97, Program for Crystal Structure Refinement, G. M. Sheldrick, 1997.
- [81] L. J. Farrugia, *J. Appl. Crystallogr.* **1999**, *32*, 837–838.
- [82] C. B. Hübschle, G. M. Sheldrick, B. Dittrich, *J. Appl. Crystallogr.* **2011**, *44*, 1281–1284.
- [83] Diamond 4.3.2, K. Brandenburg, Crystal Impact GbR, 1997–2017.
- [84] W. Kohn, L. J. Sham, *Phys. Rev. A* **1965**, *140*, 1133–1138.
- [85] A. D. Becke, *Phys. Rev. A* **1988**, *38*, 3098–3100; A. D. Becke, *J. Chem. Phys.* **1993**, *98*, 5648–5652; C. Lee, W. Yang, R. G. Parr, *Phys. Rev. B* **1988**, *37*, 785–789.
- [86] Gaussian 09 Revision D.01, M. J. Frisch, G. W. Trucks, H. B. Schlegel, G. E. Scuseria, M. A. Robb, J. R. Cheeseman, V. Barone, B. Mennucci, G. A. Petersson, H. Nakatsuji, M. Caricato, X. Xi, H. P. Hratchian, A. F. Izmaylov, J. Bloino, G. Zheng, J. L. Sonnenberg, M. Hada, M. Ehara, K. Toyota, R. Fukuda, J. Hasegawa, M. Ishida, T. Nakajima, Y. Honda, O. Kitao, H. Nakai, T. Vreven, J. J. A. Montgomery, J. E. Peralta, M. B. F. Ogliaro, J. J. Heyd, E. Brothers, K. N. Kudin, V. N. Staroverov, R. Kobayashi, J. Normand, K. Raghavachari, A. Rendell, J. C. Burant, S. S. Iyengar, J. Tomasi, M. Cossi, N. Rega, J. M. Millam, M. Klene, J. E. Knox, J. B. Cross, V. Bakken, C. Adamo, J. Jaramillo, R. Gomperts, R. E. Stratmann, O. Yazyev, A. J. Austin, R. Cammi, C. Pomelli, J. W. Ochterski, R. L. Martin, K. Morokuma, V. G. Zakrzewski, G. A. Voth, P. Salvador, J. J. Dannenberg, S. Dapprich, A. D. Daniels, Ö. Farkas, J. B. Foresman, J. V. Ortiz, J. Cioslowski, D. J. Fox, Gaussian, Inc., 2009. R. Nast, *Coord. Chem. Rev.* **1982**, *47*, 89–124; R. Buschbeck, P. J. Low, H. Lang, *Coord. Chem. Rev.* **2011**, *255*, 241–272.

Entry for the Table of Contents

FULL PAPER



Johannes Landmann, Jan A. P. Sprenger, Philipp T. Hennig, Rüdiger Bertermann, Matthias Grüne, Frank Würthner, Nikolai V. Ignat'ev, and Maik Finze*

Page No. – Page No.

Perfluoroalkyltricyanoborate and Perfluoroalkylcyanofluoroborate Anions: Building Blocks for Low-viscosity Ionic Liquids

Unique perfluoroalkylcyanoborate ionic liquids exhibiting high thermal, chemical and electrochemical stabilities and providing low viscosities and high conductivities were developed.